

The banner features a background of a sunset or sunrise with a lighthouse on the left and a stylized particle beam or light trail on the right. The text is centered and reads:

The 11th Advanced Accelerator Concepts Workshop 2004

*Stony Brook, NY June 21-26 Organized by Stony Brook University and the Brookhaven National
Laboratory's Accelerator Test Facility*

Gas Lasers for strong field applications

tutorial

Igor Pogorelsky

Accelerator Test Facility, BNL

MOTIVATION

- ❖ Why are we talking today about gas lasers?
Indeed, 99% of publications on advance acceleration or broader high power laser scientific applications consider solid state lasers.
- ❖ Meantime CO₂ gas lasers enabled:
 - the first laser beatwave acceleration
 - ICA and IFEL electron acceleration
 - the first and only staged and monoenergetic laser accelerator
 - the strongest Thomson scattering source
- ❖ All above with just two gas laser facilities operating for this kind of experiments
- ❖ Developing practical alternative solutions for particle accelerators and radiation sources requires taking all the best from both **solid state** and **gas laser** technologies and pushing these technologies up in power, rep. rate, etc.

OUTLINE

- ❖ GAS LASERS:
 - spectral range from UV to Far-IR
 - kW and even MW of average power
 - wall plug efficiency up to 70%
- ❖ Active medium:
 - atoms, molecules, excimers
- ❖ Variety of pumping schemes:
 - electric discharge, electron beams,
 - optical and chemical pumping

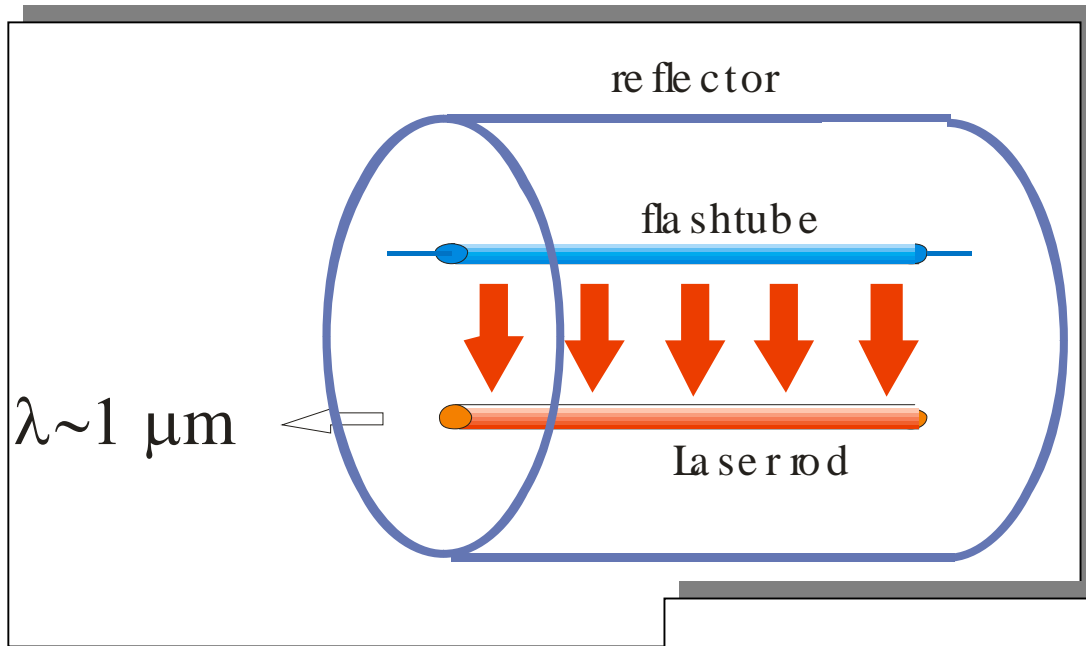
O U T L I N E (closer to the point)

- ❖ We narrow our scope to gas lasers capable to produce pico- and femtosecond pulses with relativistically strong normalized fields $a > 1$ and high repetition rate.
- ❖ We will review several ongoing projects in this field.
- ❖ Special attention is given to picosecond CO₂ lasers that proved to be a valuable tool for strong-field physics applications.
- ❖ Finally, we will analyze possibilities for generating CO₂ laser pulses of the Petawatt peak power and a few cycles long.

Typical Parameters of Solid State and CO₂ Lasers

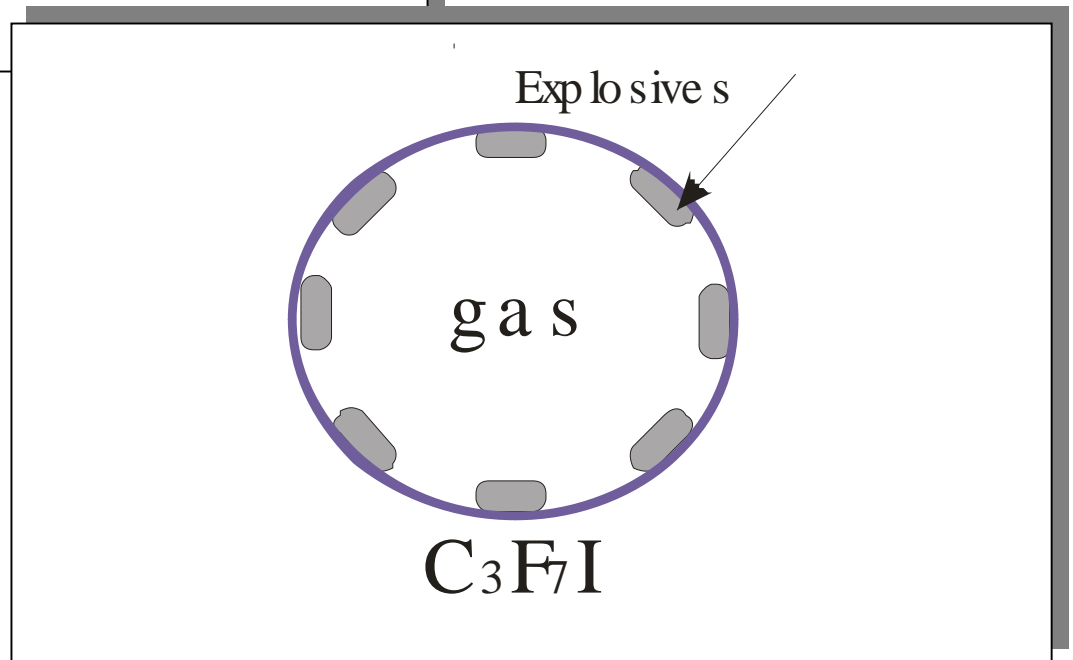
PARAMETER	Solid State	10-atm CO ₂
Host matrix density (cm ⁻³)	10 ²³	10 ²⁰
Active particle density (cm ⁻³)	10 ²⁰	10 ¹⁹
Photon energy (eV)	1	0.1
Stored energy (J/cm ³)	1	0.02
Gain (%/cm)	~50	3-4
Active volume (cm ³)	100	10,000
Output energy (J)	100	100
Bandwidth (THz)	5-50	1
Average power (kW)	1	10

Lasers with Optical Pumping

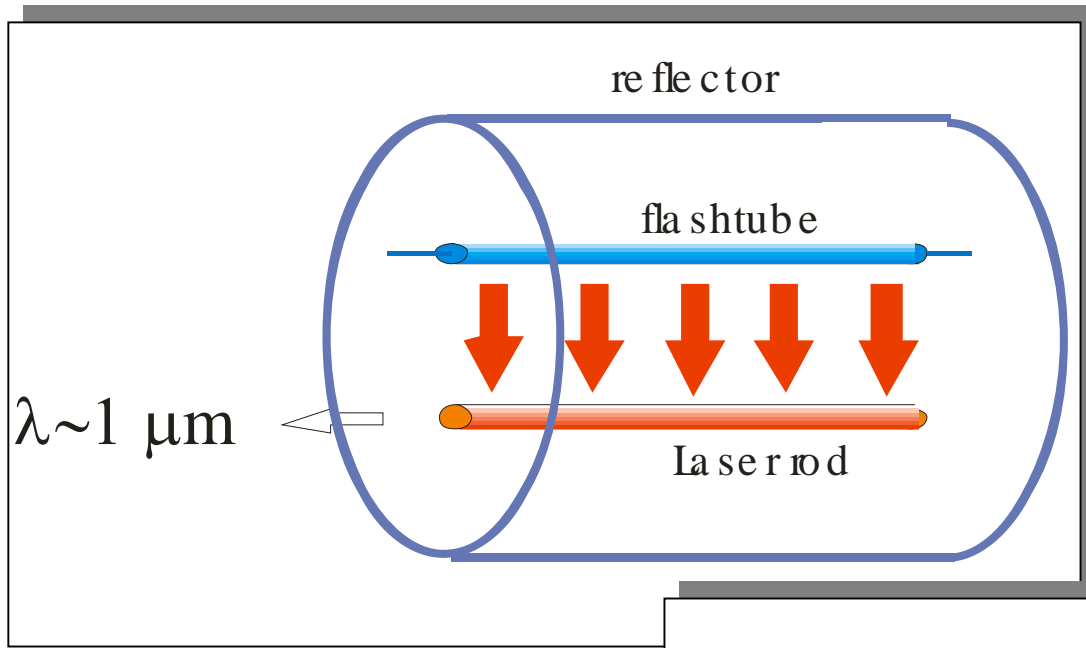


Solid State Laser

Photodissociation
Iodine Laser

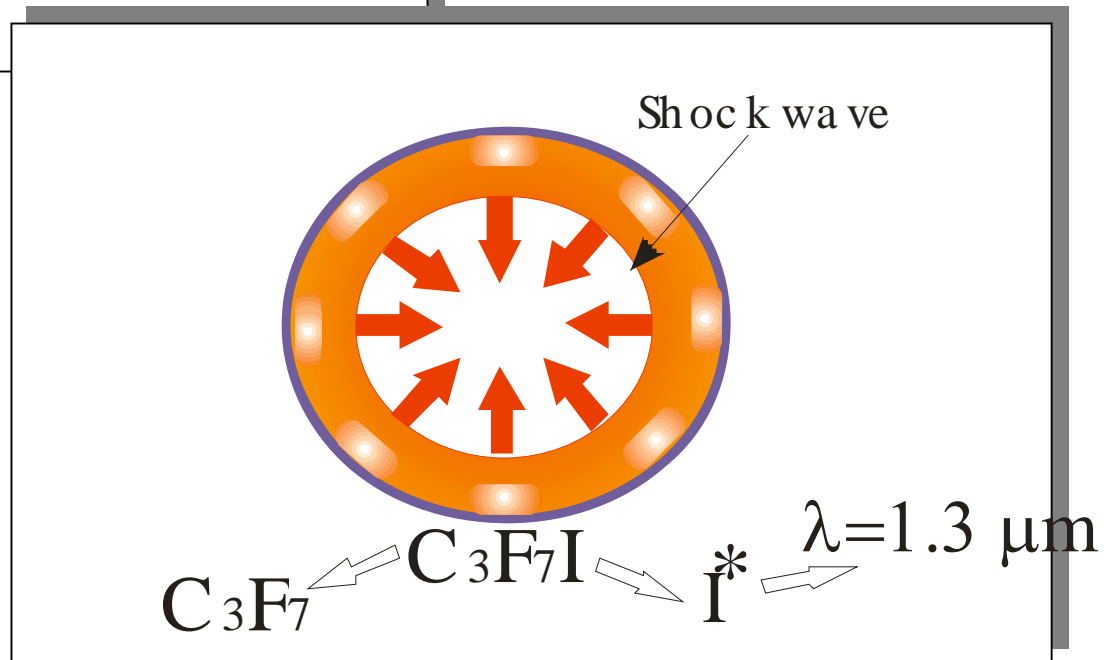


Lasers with Optical Pumping

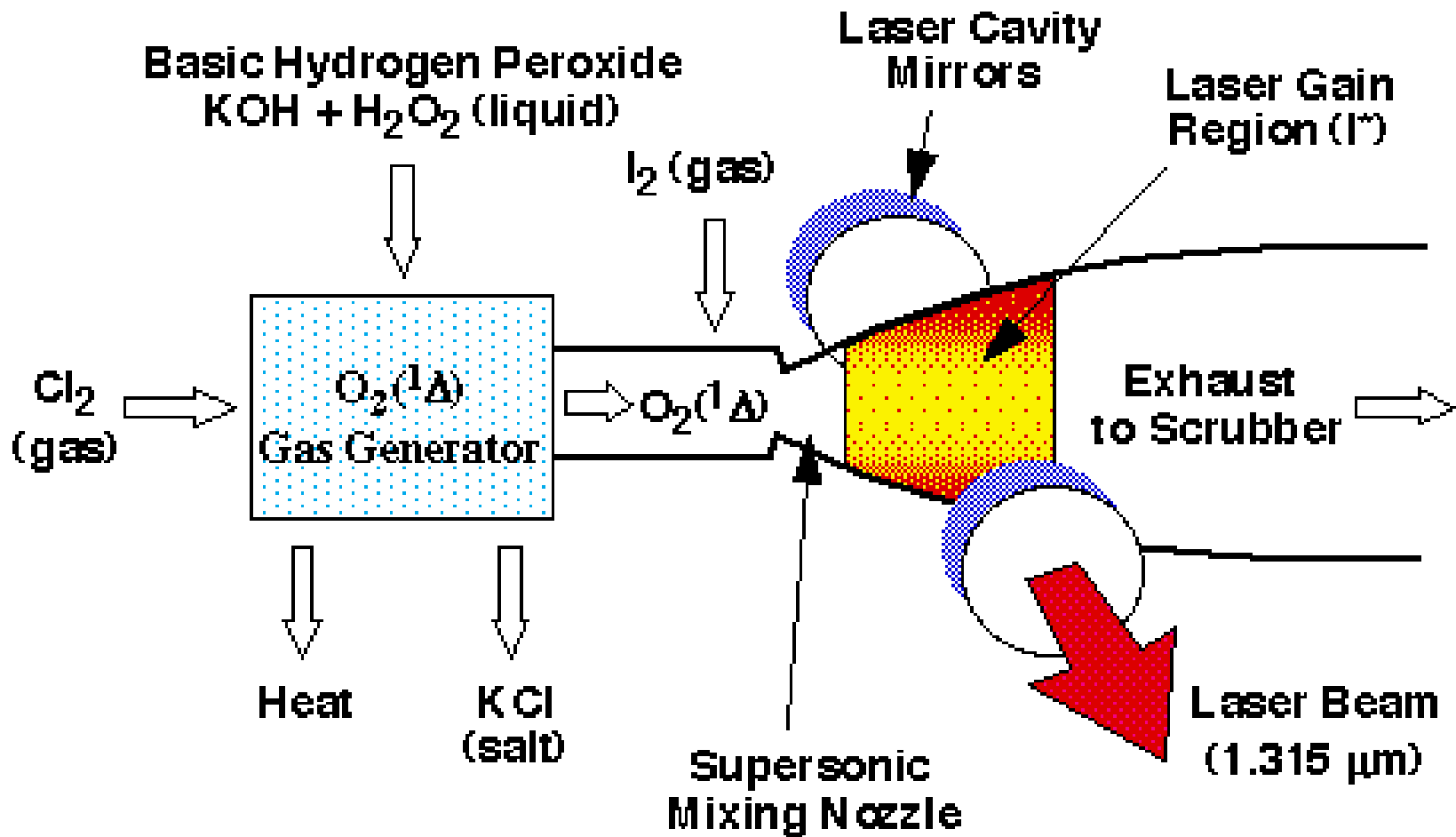


Solid State Laser

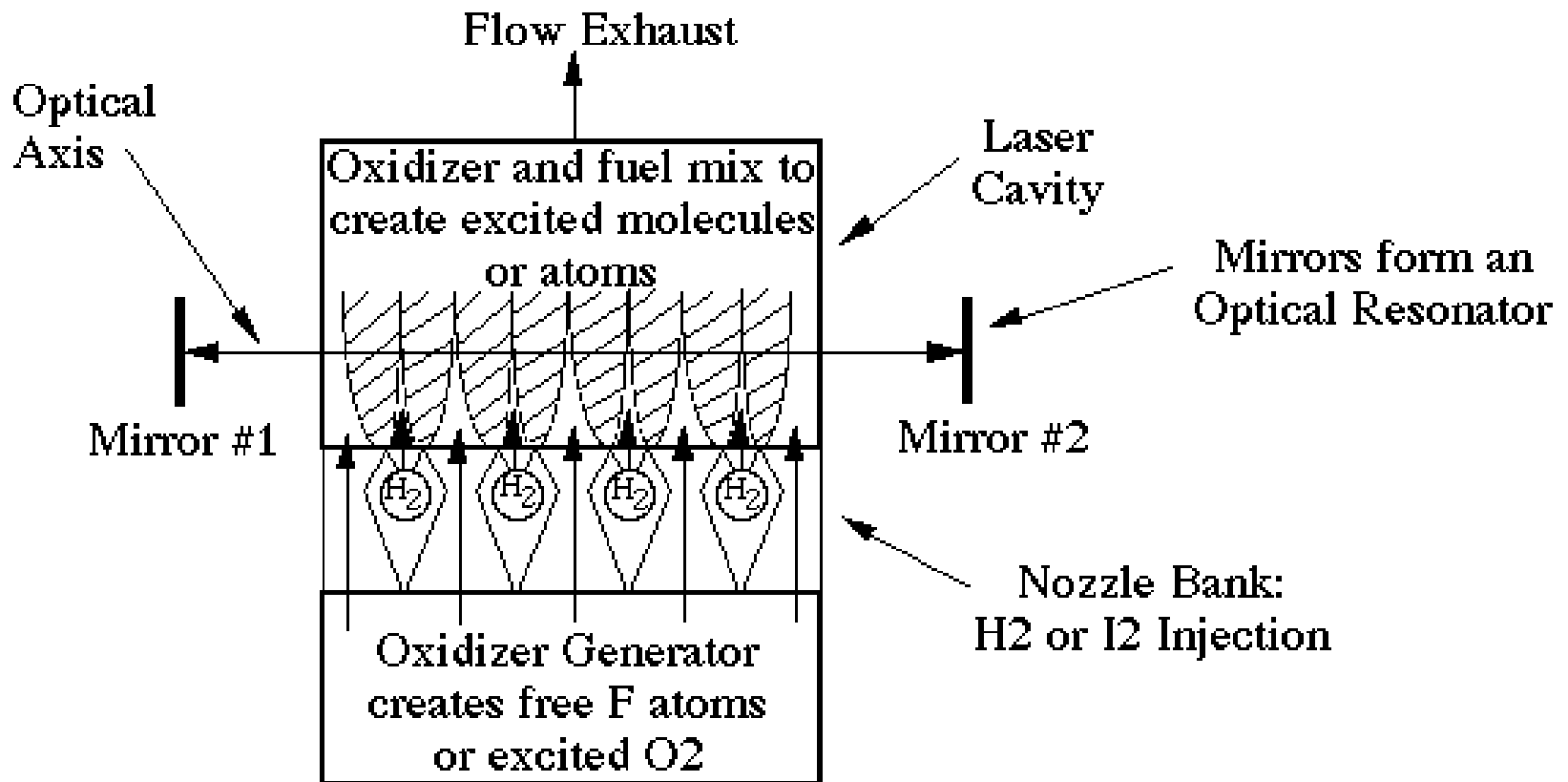
Photodissociation
Iodine Laser



COIL - Chemical Oxygen Iodine Laser

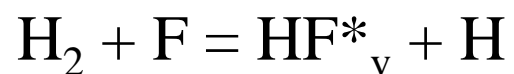
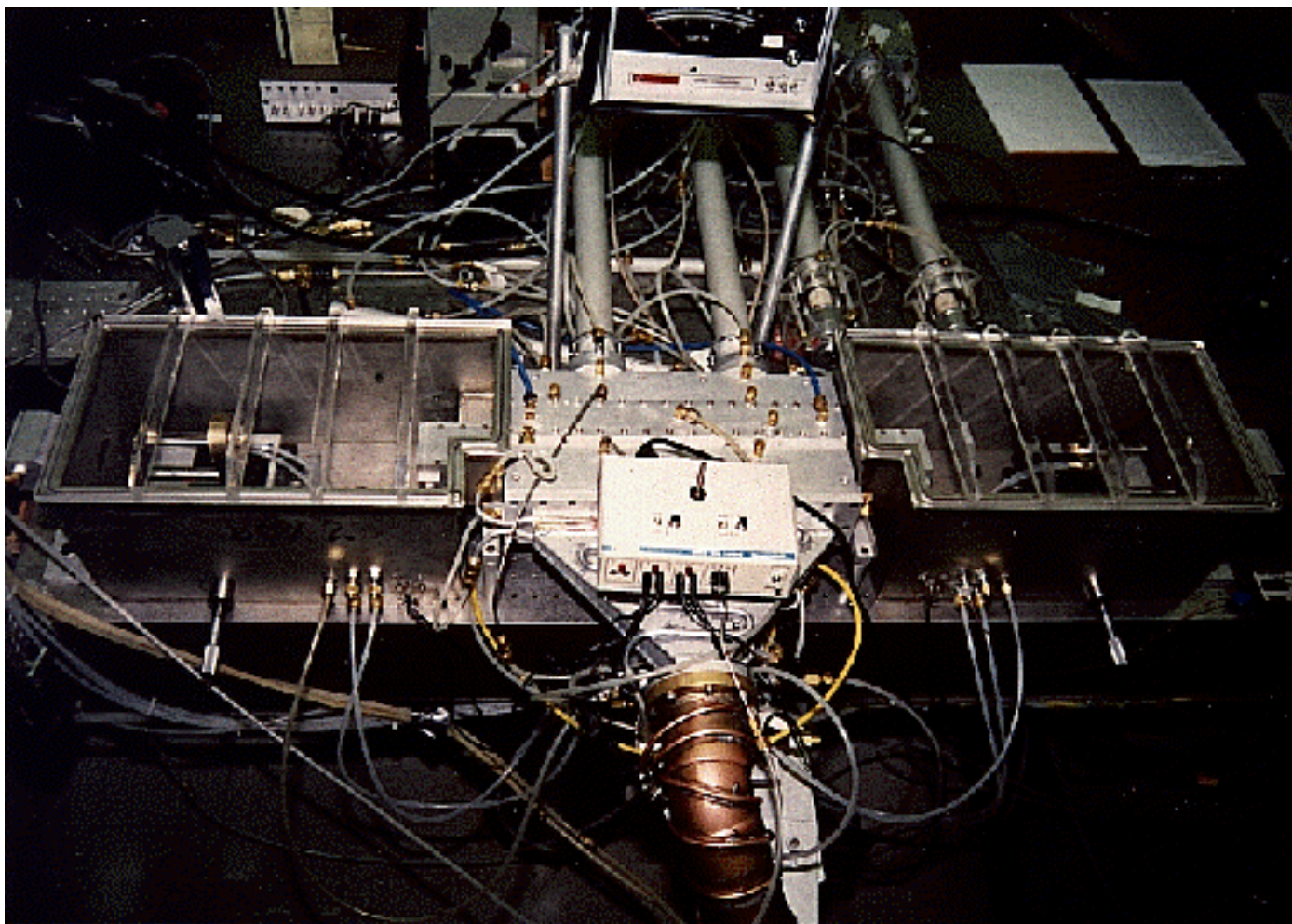


Chemical laser



- An HF chemical laser uses F as the oxidizer and H₂ as the fuel
- A COIL device uses excited O₂ as the oxidizer and I₂ as the fuel

Chemical laser



COIL in flight

(chemical oxygen iodine laser) (cartoon)

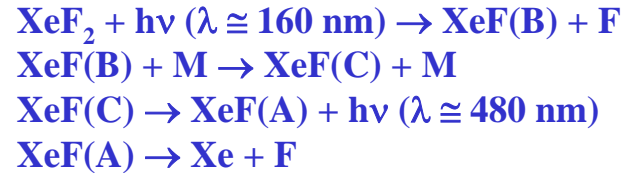
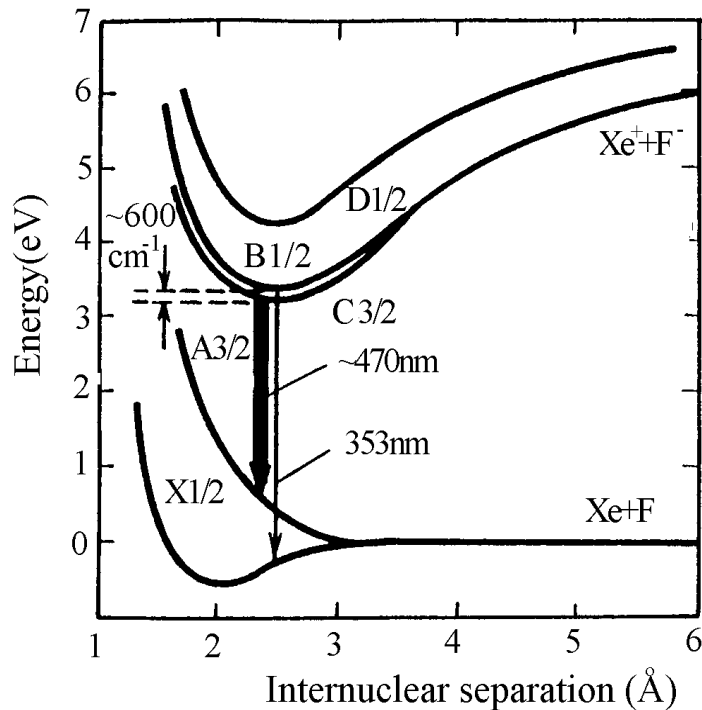
AIRBORNE LASER
system



Gas lasers capable to high average power and repetition rate

	Excimer, discharge or photopump	Iodine, photo- chemical	HF, chemical	CO ₂ (CO), discharge
Wavelength [μm]	0.2-0.3	1.3	3-4	9-10 (4-5)
Average Power [kW]	1	10	1	50
Repetition Rate [kHz]	0.1-10	10	0.1	1
Wall-Plug Efficiency [%]	15	30	180	30 (70)
Gas Consumption	closed loop	kg/min	kg/min	closed loop
Min. Pulse (Theory) [ps]	0.03	1000	100	0.15

Photochemical XeF excimer laser



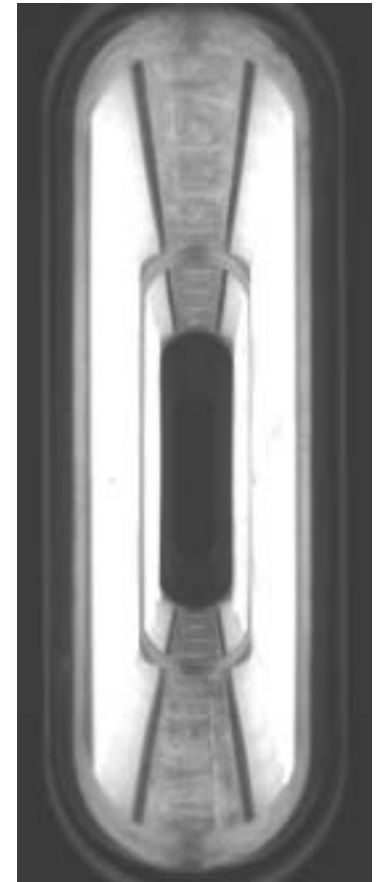
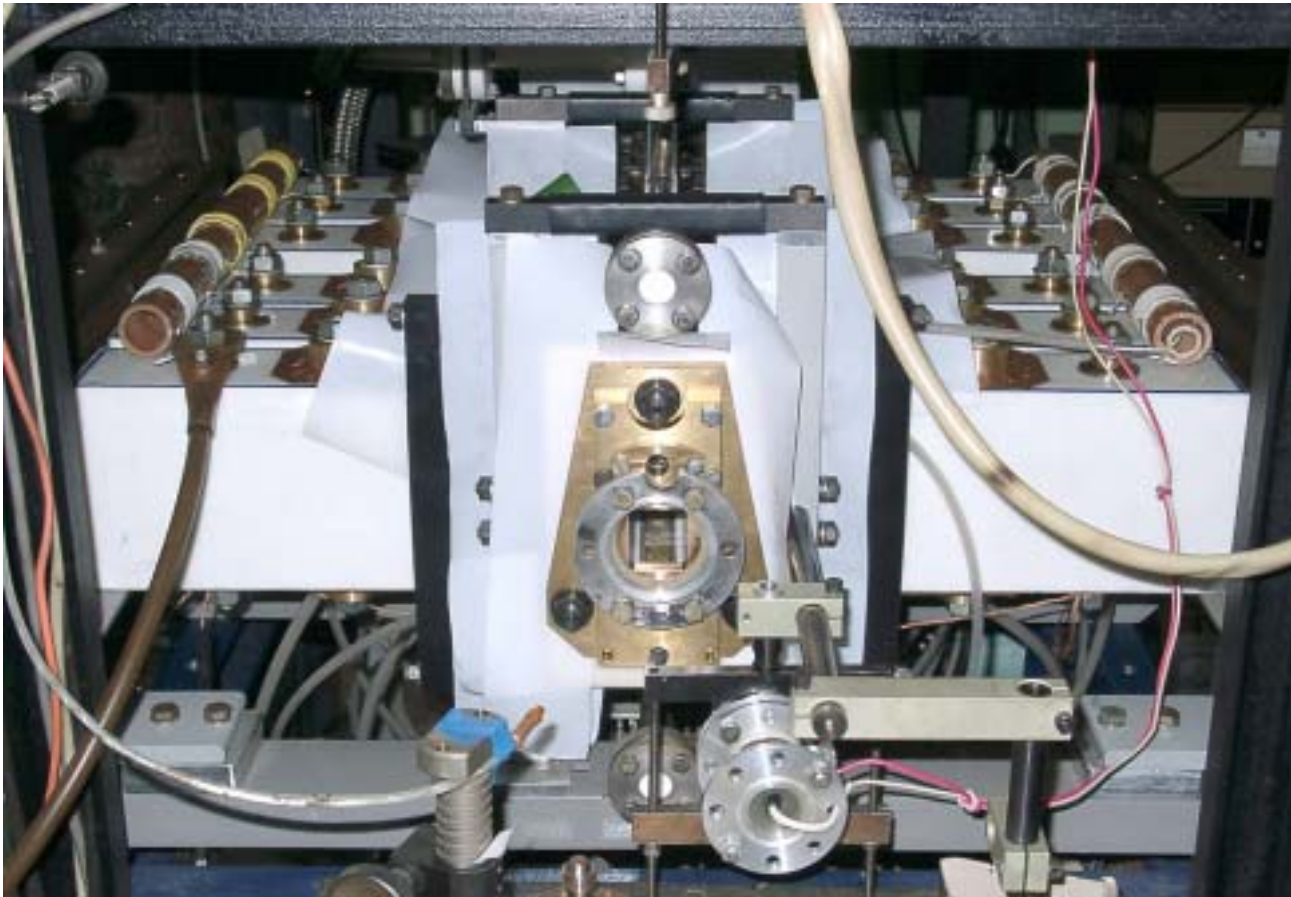
*Bandwidth 100 nm \Rightarrow
Transform limited pulse duration
10 fsec*

Up to 1 kJ energy demonstrated

*Wavelength match to frequency doubled
Ti:Sa*

Courtesy of D. Mikheev
P.N.Lebedev Physical Institute
Quantum Radiophysics Division
Photochemical Processes Laboratory

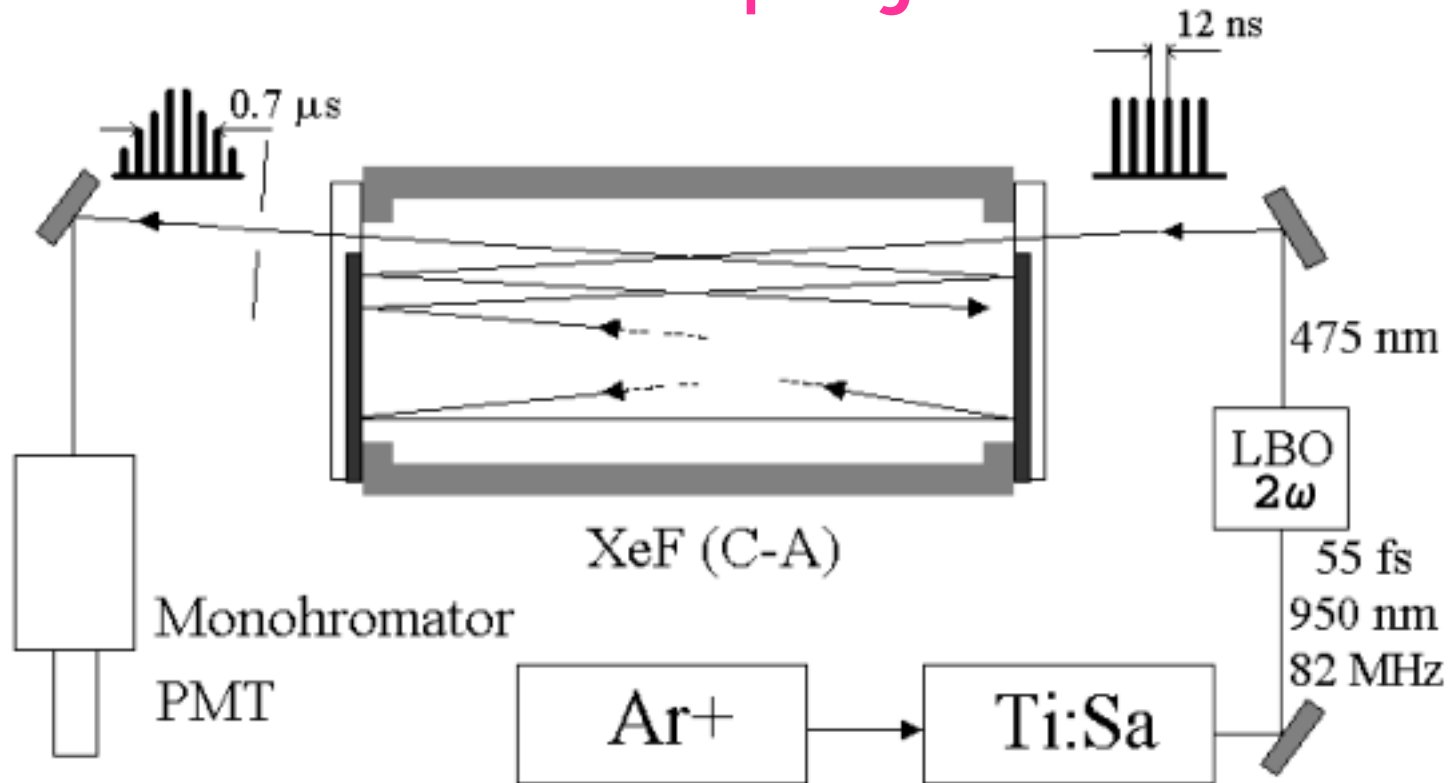
Photochemical XeF amplifier of fsec optical pulses



Courtesy of D. Mikheev
P.N.Lebedev Physical Institute
Quantum Radiophysics Division
Photochemical Processes Laboratory

Multi-channel surface discharge
active medium size $3 \times 11 \times 50 \text{ cm}^3$

100 TW project

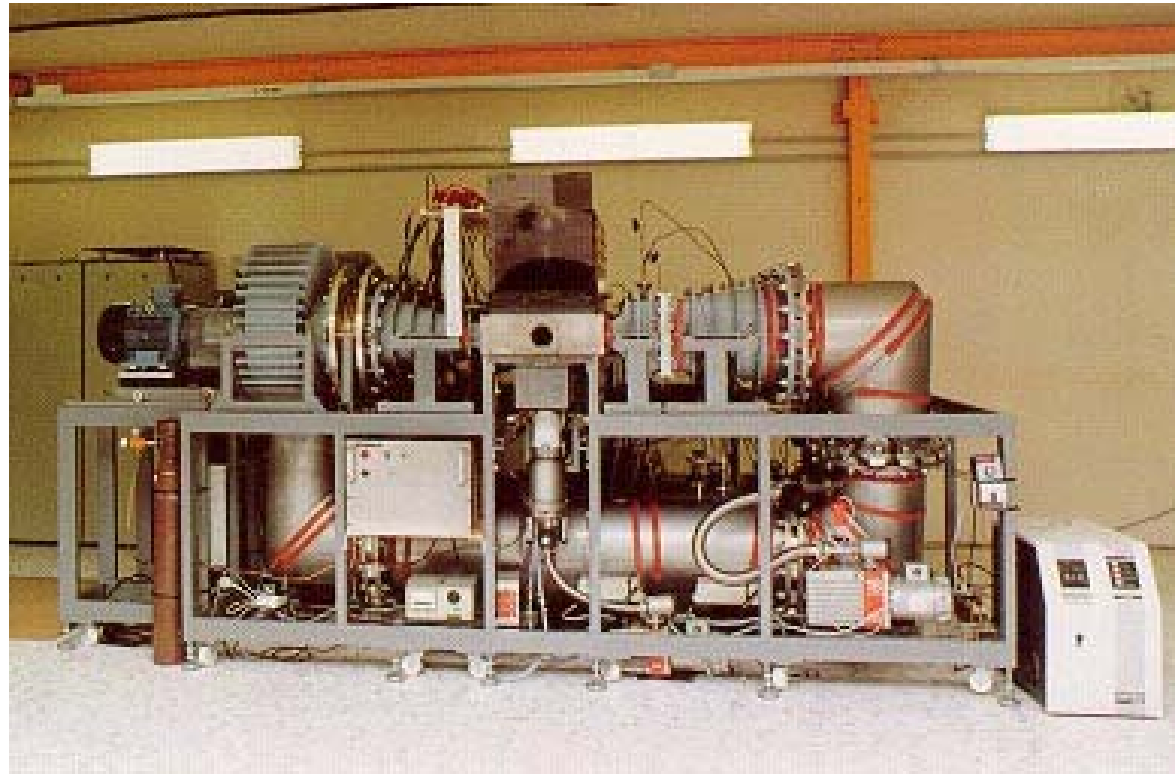


Achieved amplification $\times 40$ in 39 passes
Required: 1.6×10^3 in 78 passes
Contrast 10^{10}

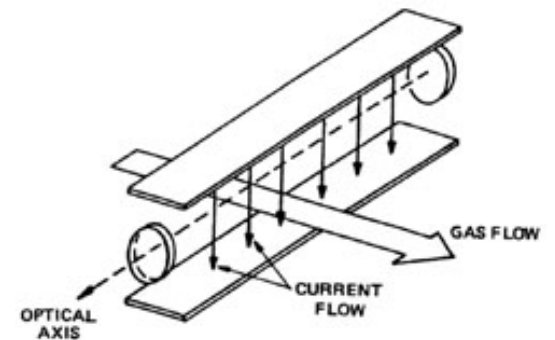
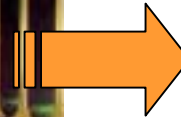
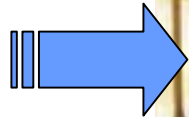
Courtesy of D. Mikheev
P.N.Lebedev Physical Institute
Quantum Radiophysics Division
Photochemical Processes Laboratory

Electrical discharge excimer laser

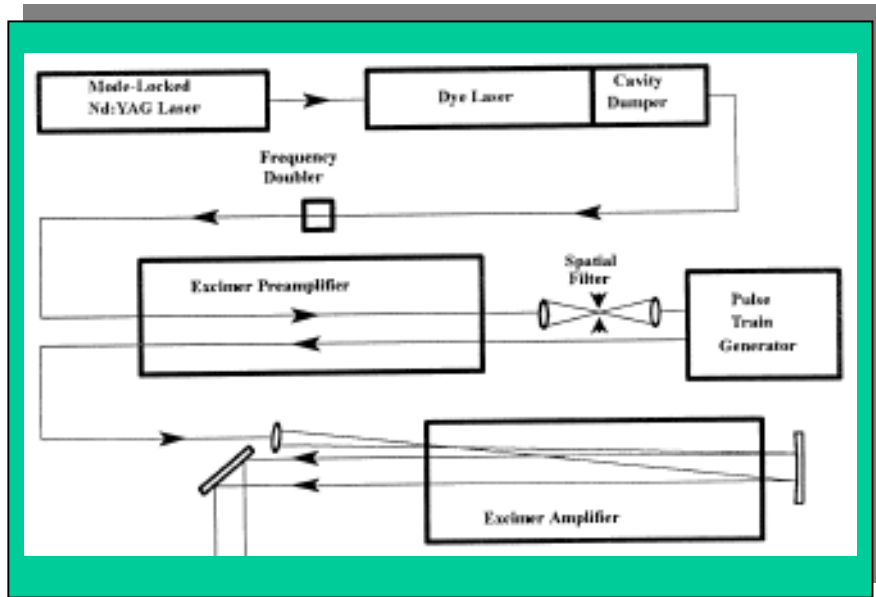
10 J per pulse,
100 Hz repetition rate,
1 kW average power



gas flow



Example of multi-stage high repetition rate excimer laser



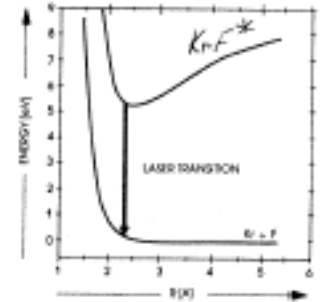
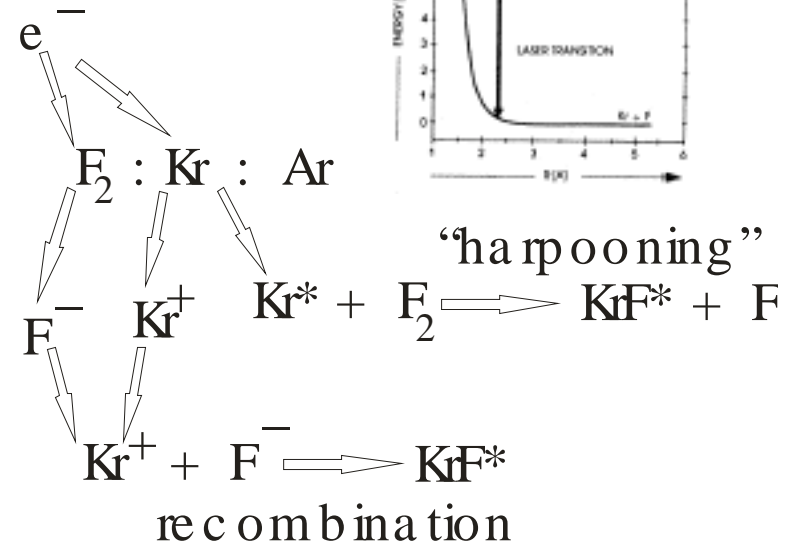
Demonstrated:

10 ps,
400 Hz x 20 pulse/train = 8 kHz rep. rate,
50 W average power

Possibility:

1 kW with SOPRA-class laser amplifier
Bandwidth 20 THz allows 50 fs amplified
without stretching

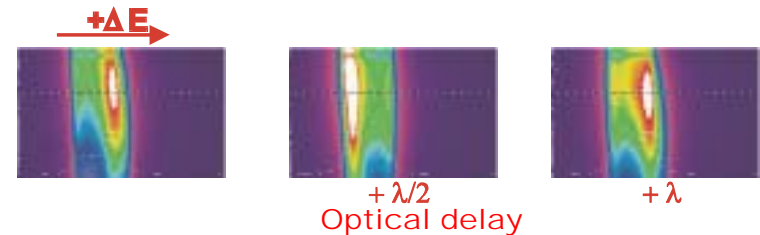
KrF laser



Benefits of using long-wavelength ($\lambda=10\mu\text{m}$) CO_2 laser:

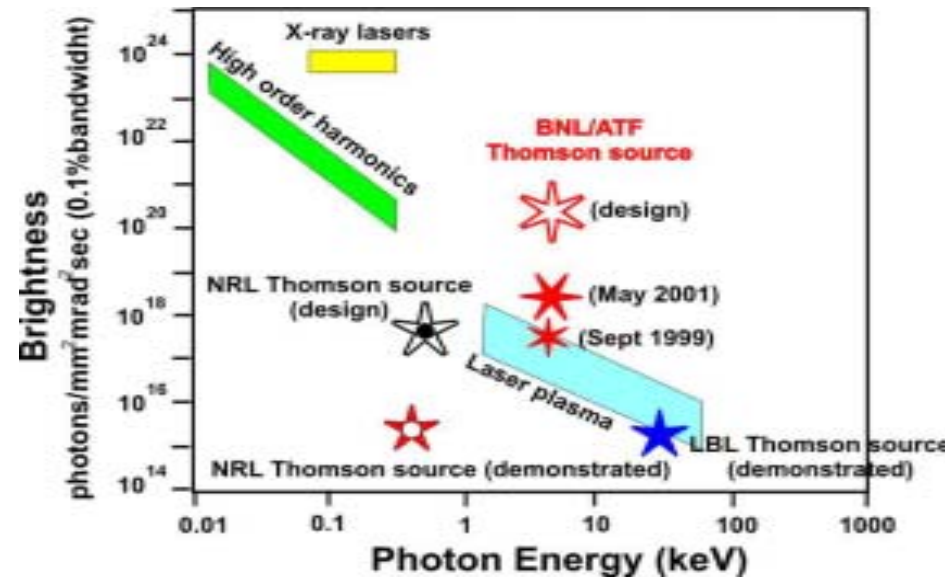
- Combines advantages of high-quality conventional RF accelerators and high-gradient optical accelerators with $\lambda \approx 1 \mu\text{m}$
 - favorable phasing
 - structure scaling.

Illustrated by STELLA - the first two-stage laser accelerator

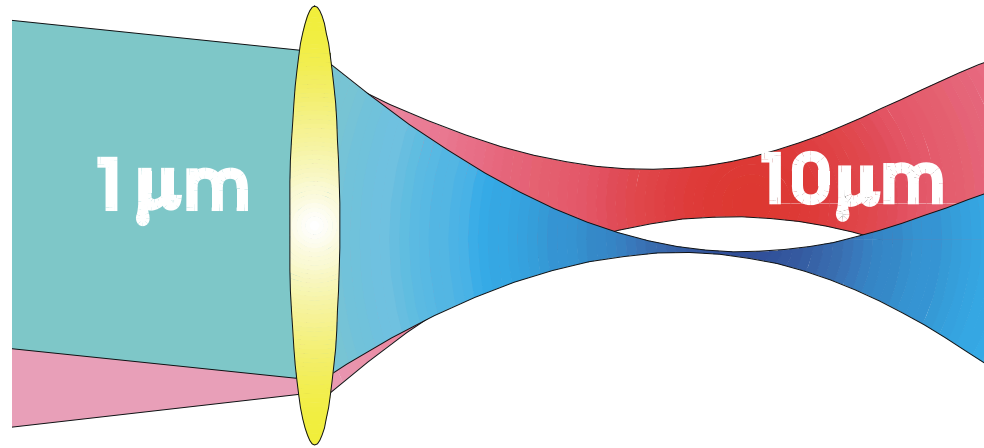


- Ponderomotive potential that controls x-ray production, plasma wake generation and other strong-field phenomena is proportional to λ^2 .

Illustrated by Thomson scattering experiment – presently the brightest Thomson x-ray source.



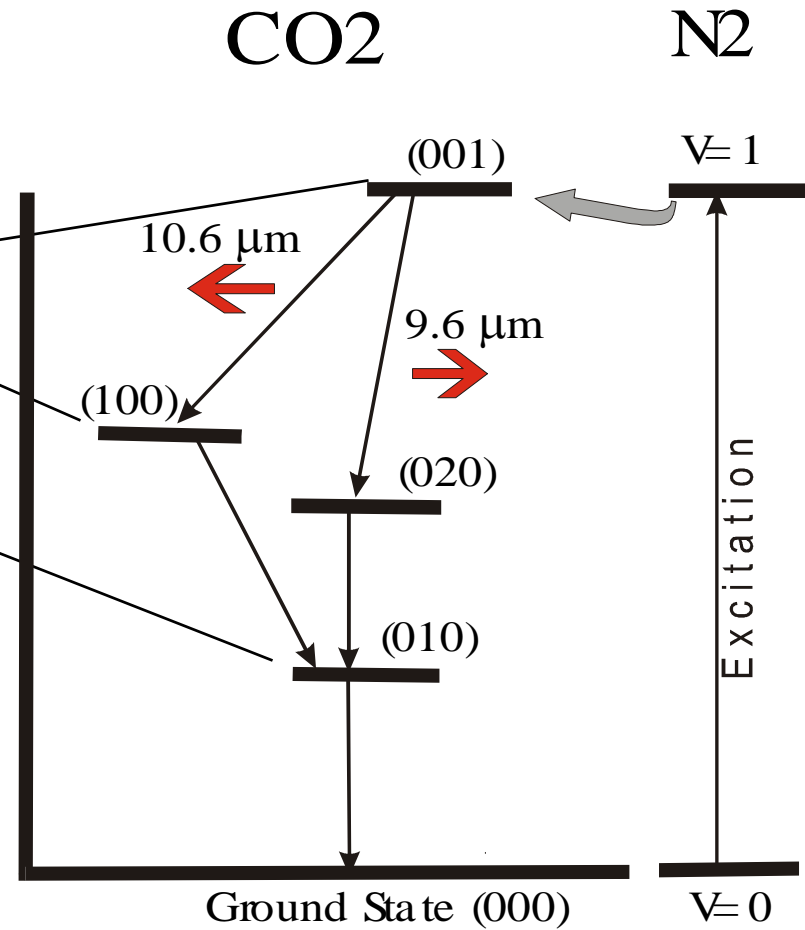
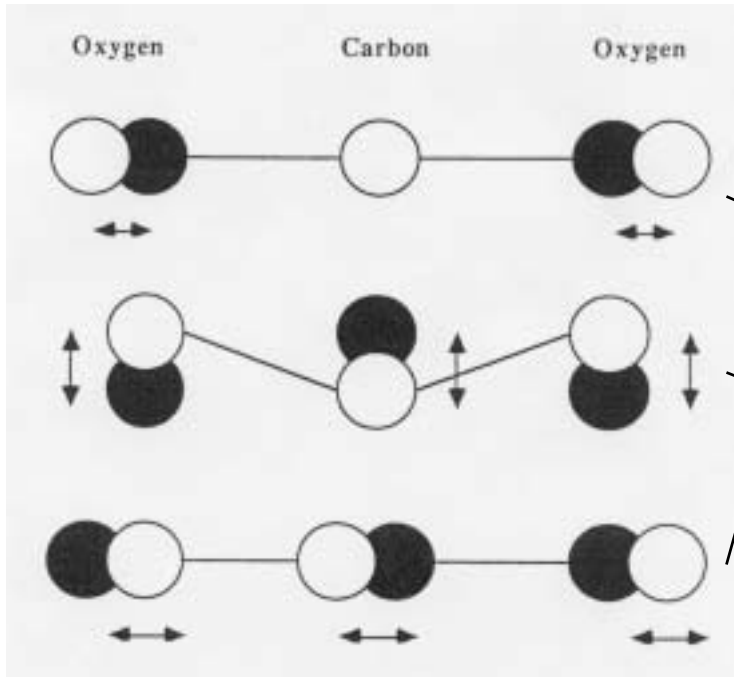
...but $\lambda=1 \mu\text{m}$ permits tighter focusing (assuming $w_0 \sim \lambda$) !



However:

- ◆ Interacting with e-beam you do not want to focus laser tighter than e-beam (decreases acceleration quality and x-ray yield). CO₂ laser focusing is sufficient to interact with low-emittance e-beams.
- ◆ In volumetric interactions ten times tighter focus of the 1 μm laser results in 1000 times smaller interaction volume where we can see an equivalent effect. This will proportionally reduce the process yield.
- ◆ Thus, 1 TW CO₂ laser in certain cases is equivalent to 100 TW solid state laser.

CO₂ Laser



- CO₂ vibrational modes
- Discharge excites N₂; N₂ excites CO₂
- Radiation transitions between vibrational levels

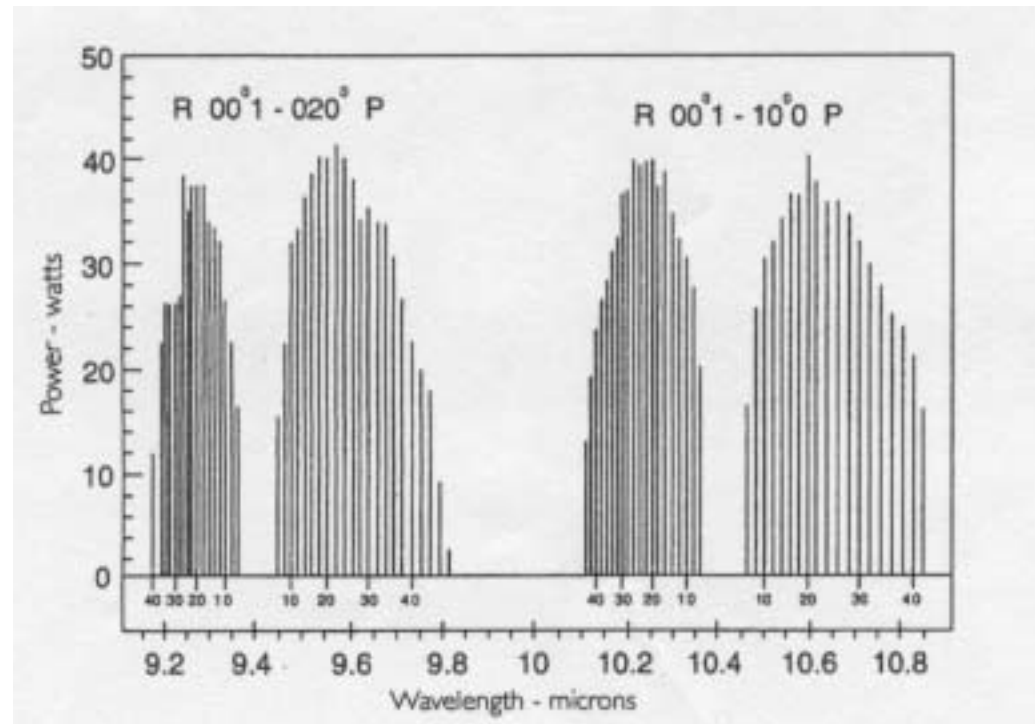
Rotational CO₂ Laser Lines

- Vibrational bands are composed of a transitions between rotational sublevels.
- Selection rules for symmetric CO₂ molecules allow only transitions where the rotational quantum number J changes by ± 1 .
- They constitute correspondingly P - and the R -branches of vibrational bands with the central lines defined by expressions:

$$\nu_P = \nu_0 + B_1 J(J + 1) - B_2 (J + 1)(J + 2)$$

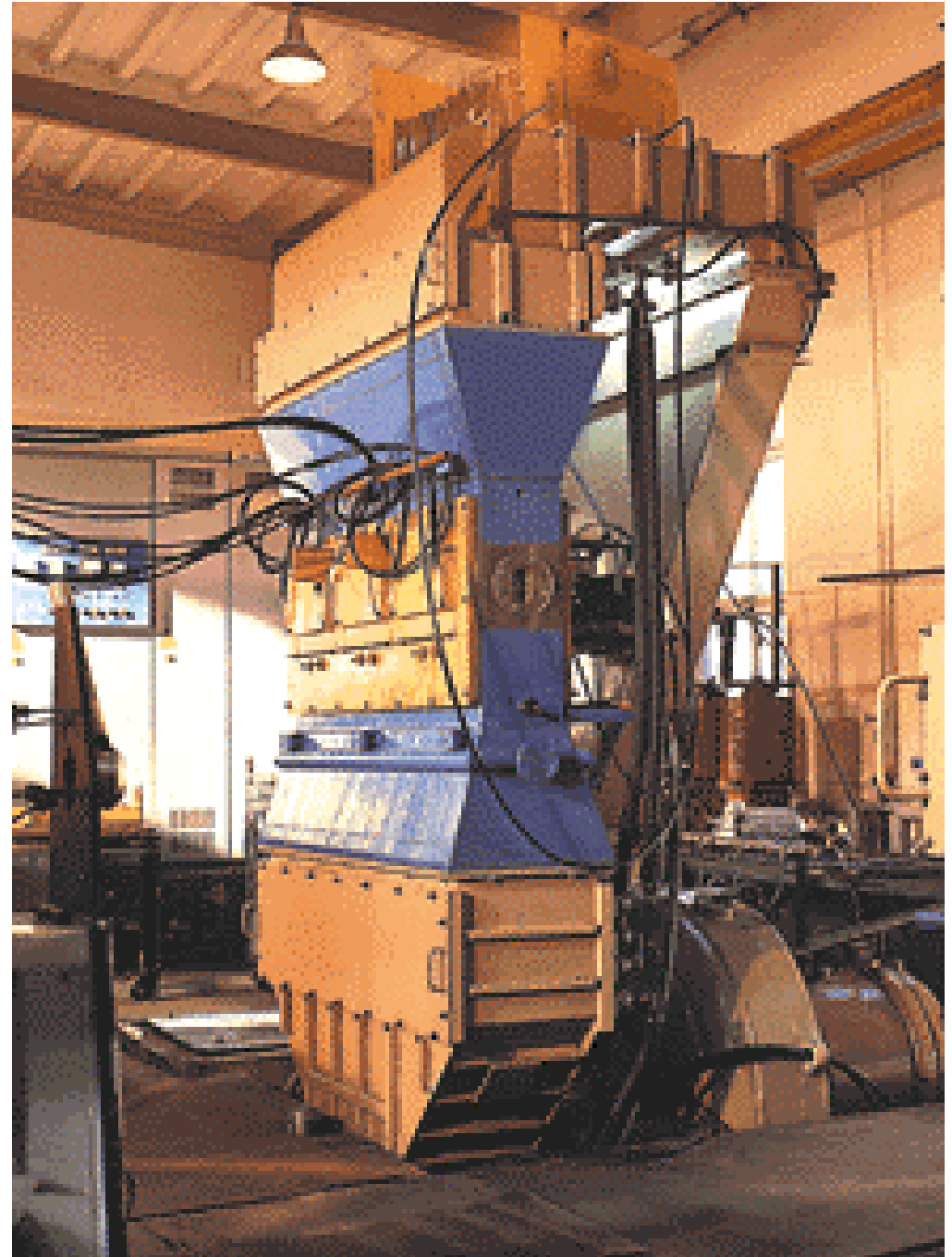
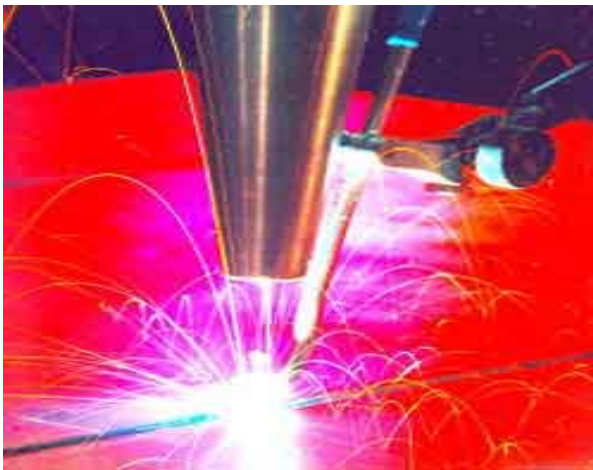
Grating selects operating line

$$\nu_R = \nu_0 + B_1 J(J + 1) - B_2 (J - 1)J$$



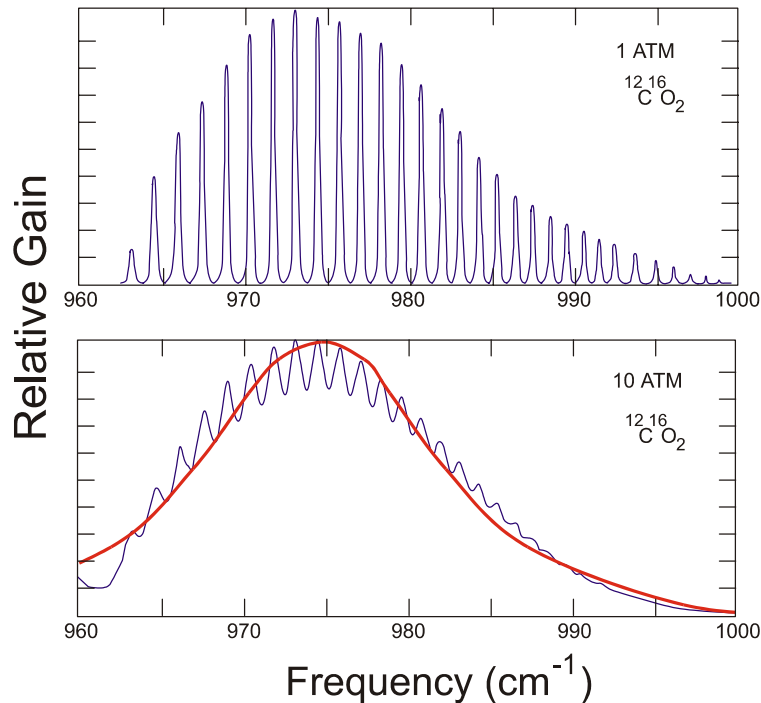
At the normal discharge temperature the maximum line strength is at $J \sim 20$ and the typical interline spacing varies between 1.4 cm^{-1} (38 GHz) for 9R-band to 1.8 cm^{-1} (55 GHz) for 10P-band. Each branch contains about 20-30 rotational lines and covers $\sim 1 \text{ THz}$ bandwidth

Industrial
CO₂ Lasers
CW-MHz- kHz-Hz
>10 kW

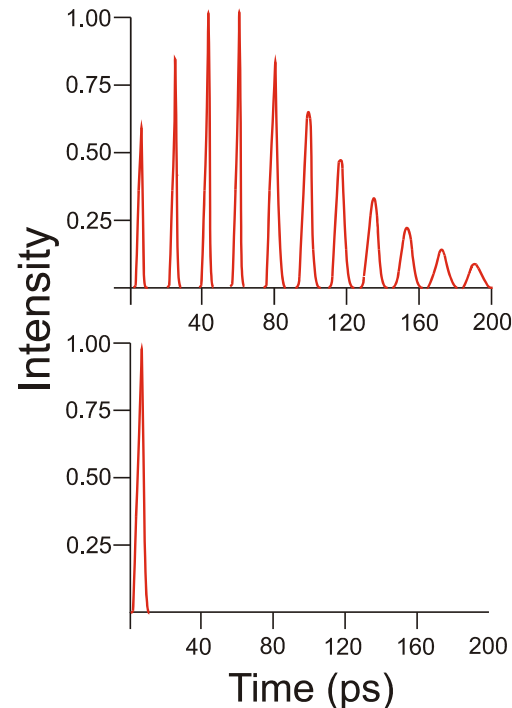


Bandwidth limited amplification of ps CO₂ laser pulses

Gain Spectrum



Amplified Picosecond Pulse

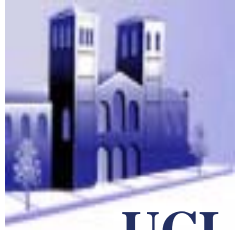


Strongly modulated rotational line structure of the CO₂ gain spectrum modifies the frequency content of picosecond pulses, changing their temporal structure.

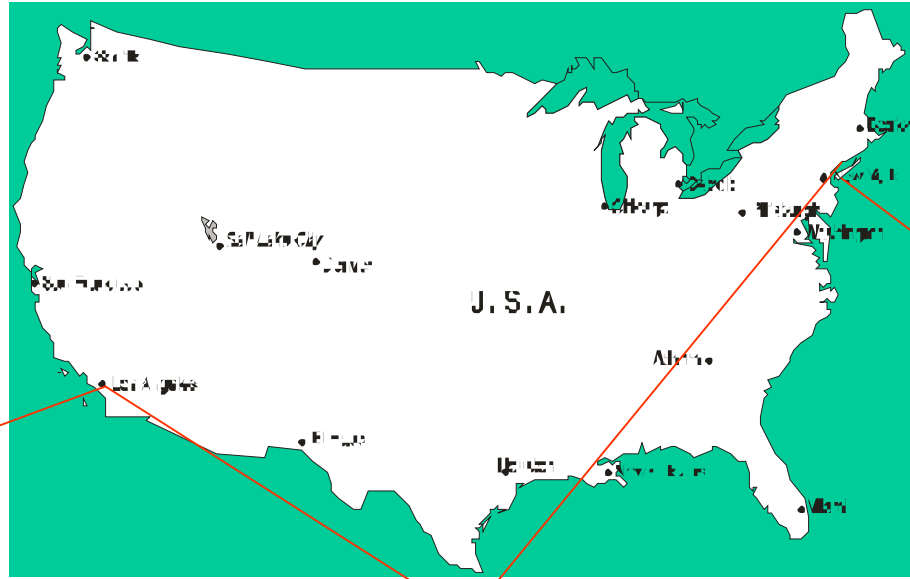
At 10 atmospheres, collisional broadening produces overlap of the rotational lines into the 1 THz wide quasi-continuous gain spectrum, and pulses as short as 1 ps can be amplified without distortion.

- Interline spacing 40 GHz
- Pressure broadening 5 MHz/torr
- Total bandwidth 1 THz
- Saturation intensity $I_s = h\nu / 2\sigma\tau_R = 3\text{kW/cm}^2$
- Small signal gain $g_0 = \sigma N^* = 0.5\%/cm$
- Specific power available for extraction $g_0 \times I_s = 30\text{W/cm}^2$

CO₂ Laser Facilities for Strong-Field Physics

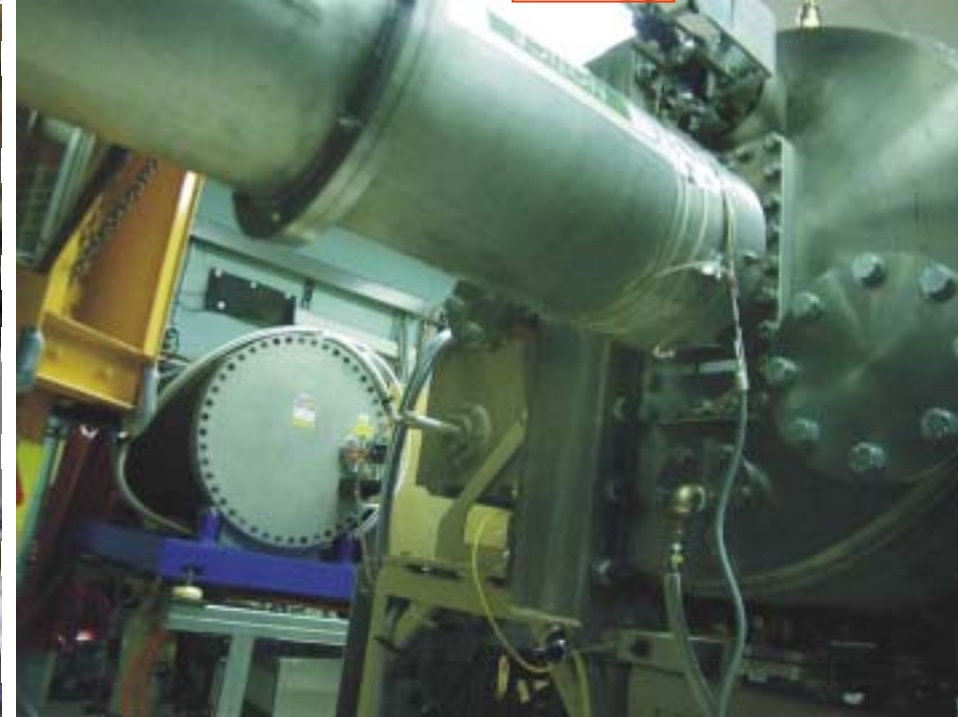
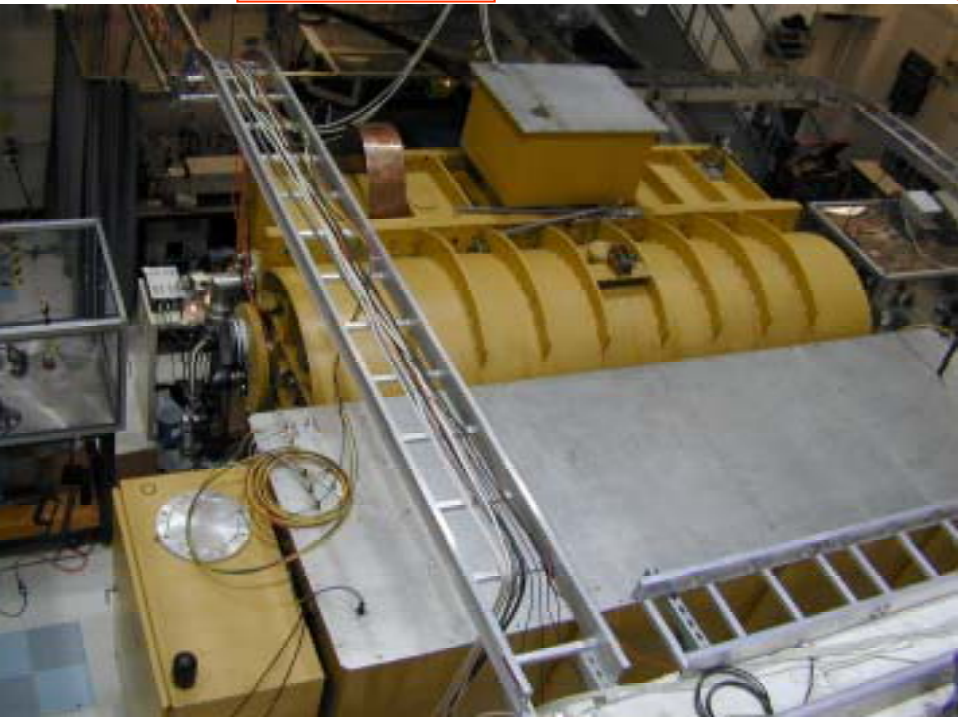


UCLA

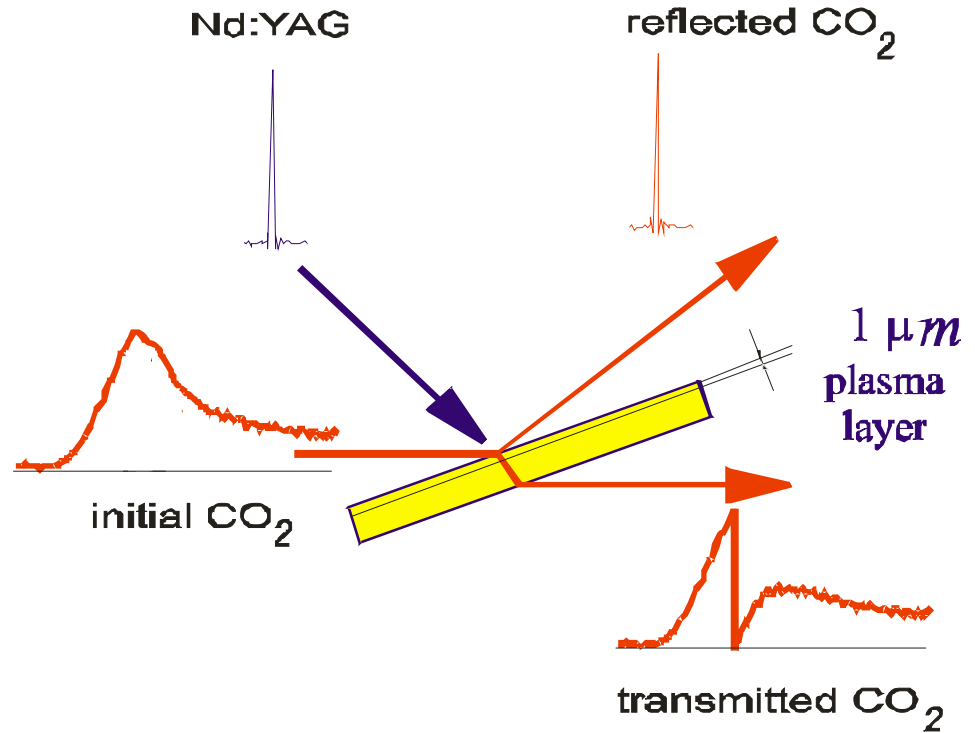
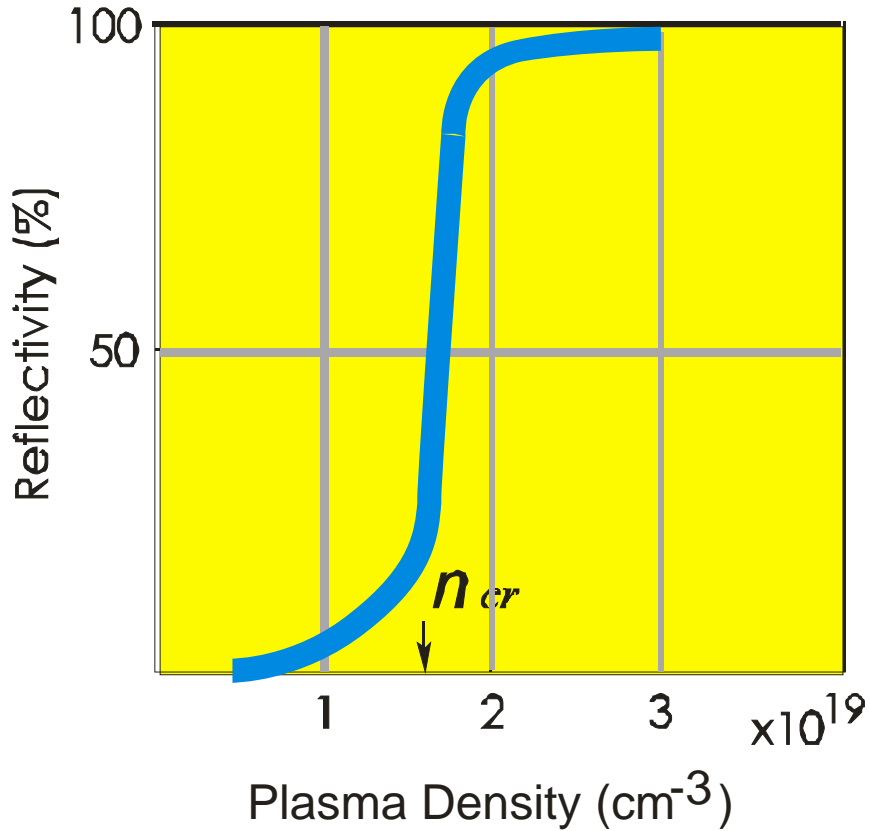


Neptune

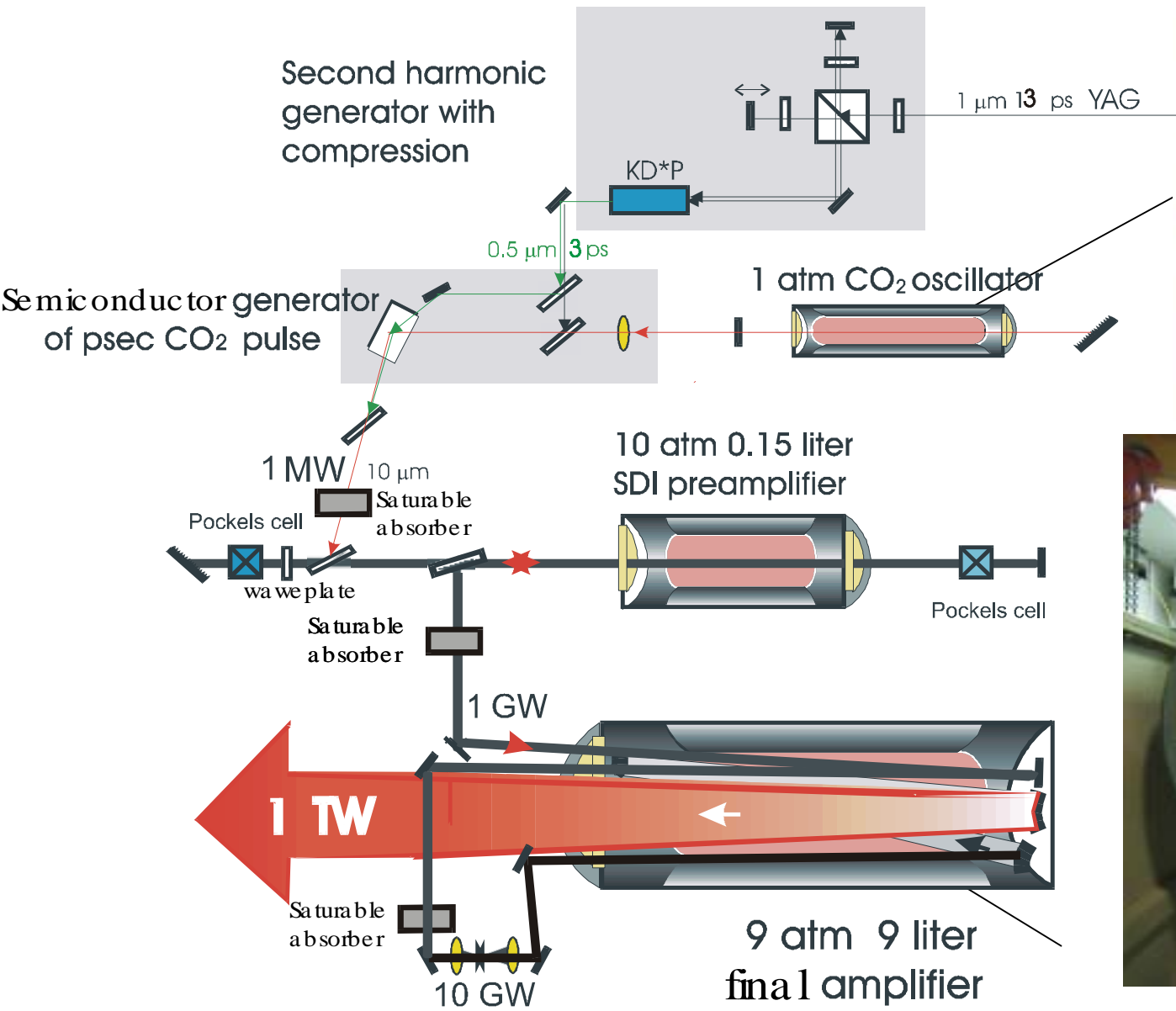
ATF



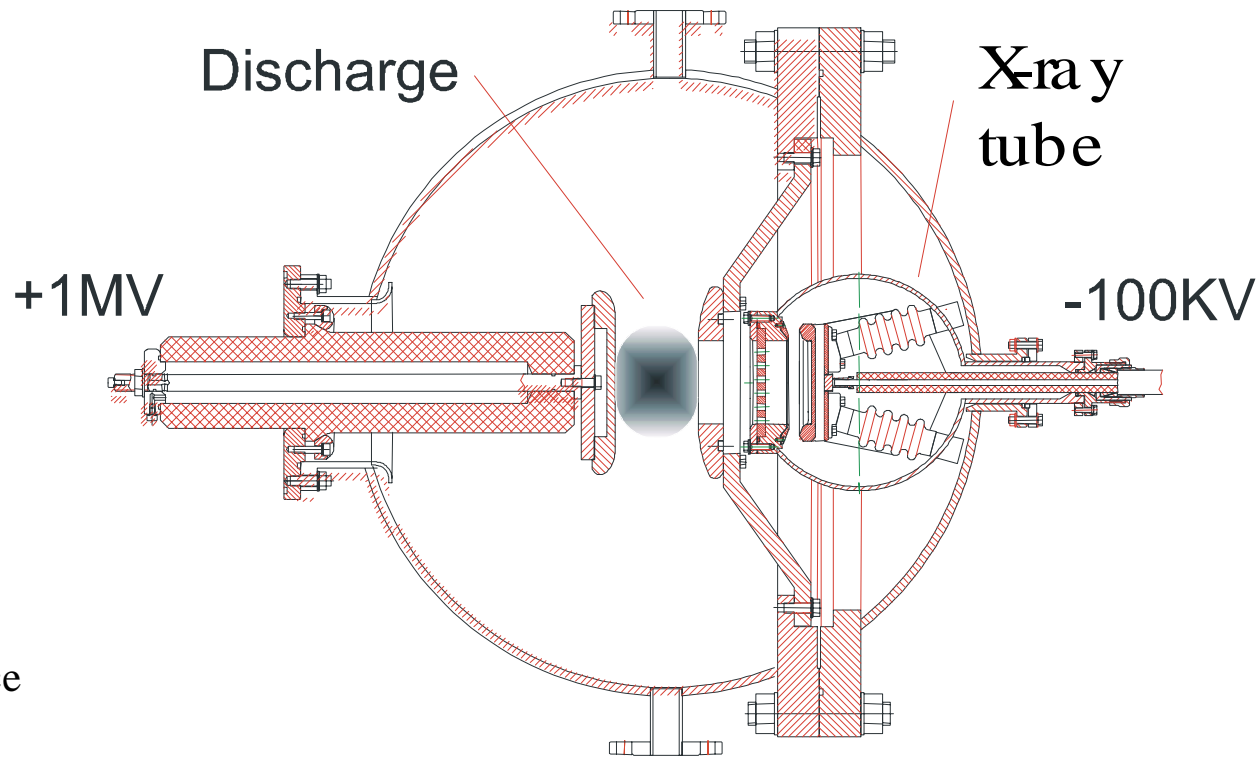
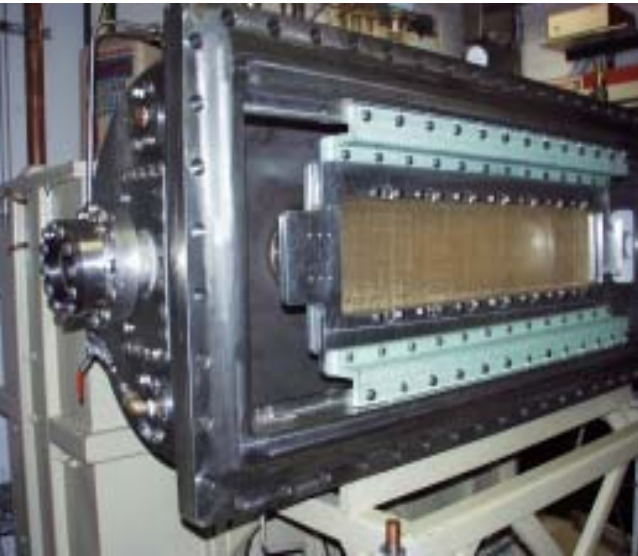
Principle of Semiconductor Optical Switching



Block diagram of ATF CO₂ laser system



High-pressure ATF laser amplifier PITER I



Amplifier cell opened for maintenance

$Pd > 25$ torr cm requires ionization source (x-ray tube)

Discharge unstable after $\tau [\mu\text{s}] \sim 3/P [\text{atm}]$ which is ~ 300 ns at 10 atm

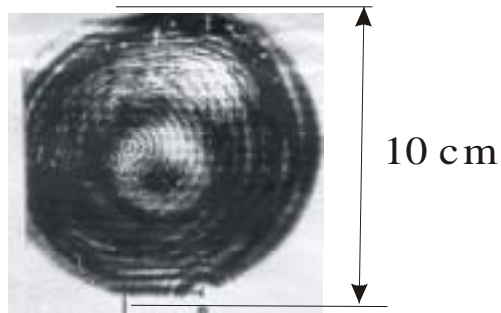
Energy load 120 J/l atm

Optical gain 2%/cm

25 ps CO₂ laser pulse measurements

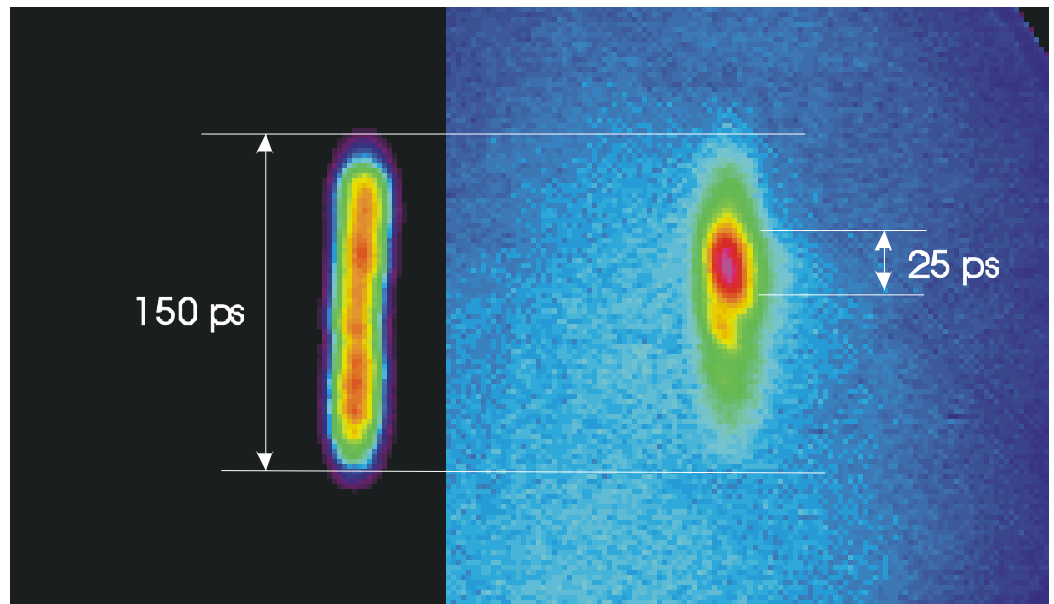
The results obtained with the 25 ps optical delay gate applied to the double-staged semiconductor optical switch prior to amplification

Output beam profile



Output energy
10 J

Autocorrelator measurements



Left - intensity distribution in 10 μm fundamental beams across the nonlinear crystal with a real time scale

Right - 2nd harmonic signal corresponding to a single-shot autocorrelation function profile

Paul Corkum (NRC) demonstrated in 1986 :

sliced 130 fs CO₂ pulses

2 ps CO₂ pulses

amplified to 0.1 TW

Generation of 130-fsec midinfrared pulses

Claude Rolland and P. B. Corkum

Division of Physics, National Research Council of Canada, Ottawa, Ontario K1A 0R6, Canada

Received June 16, 1986; accepted July 13, 1986

Infrared (IR) pulses as short as 130 fsec are generated by using semiconductor switching. Such pulses contain only ~4 optical cycles; the shortest ever achieved in the midinfrared. The measured power spectrum (7.5–10.5 μm base width) is consistent with the Fourier transform of the IR pulse.

During the past few years, new developments in the generation of ultrashort pulses have enabled researchers to study a wide variety of new phenomena.¹ Efforts aimed at developing femtosecond laser pulses has been mainly concentrated on the visible region,² and more recently on the ultraviolet.³ However, several areas such as photochemistry and solid-state physics would benefit from the availability of femtosecond pulses in other parts of the frequency spectrum. This paper reports the generation of 9.5-μm pulses as short as 130 fsec, the shortest ever achieved in the midinfrared. Such a pulse duration contains ~4 optical periods. As expected, the pulse spectrum is wide, covering the wavelength range between 7.5 to 10.5 μm.

The infrared pulses were produced by using semiconductor switching.⁴ This technique has been utilized in previous experiments to obtain low-power picosecond 10-μm radiation.^{5,6} The technique consists in illuminating a semiconductor simultaneously with a TEA CO₂ laser pulse (~100 nsec) and an ultrashort visible pulse. The electron-carrier plasma created by the high-power visible light acts as a reflective surface for the infrared (IR) radiation. A combination of two semiconductor elements, one to switch on the IR reflection followed by a second to turn off the transmission of the IR pulse, is sufficient for generating ultrashort pulses at 10 μm. The IR pulse duration can be varied continuously by using an adjustable delay line (located after the reflection switch) to modify the relative length of the visible and IR beam paths. Since the shortest pulses obtained by using this technique appeared to be limited by the visible pulse length,^{6,7} a high-power (300-μJ) ultrashort (70-fsec) pulse⁸ was used to control the switches in the femtosecond time regime.

Figure 1 shows a schematic of the experimental apparatus. A 70-μJ, 130-nsec, single longitudinal and transverse mode CO₂ laser pulse is incident upon two polycrystalline CdTe reflection switches. The switches are set at Brewster's angle (~70°) to minimize background reflection from the incoming 0.5-μm, p-polarized light. The CO₂ laser beam is focused to a diameter of ~2 mm on the CdTe slabs. In order to reduce the background reflectivity to a minimum, the switched CO₂ radiation is collected from a Ge sialon¹¹ and then passed through a wire-grid polarizer that transmits only the p-polarized radiation. A signal-to-background power ratio of ~10³:1 is obtained before the transmission switch.

The transmission switch consists of a thin Si wafer (300 μm) located at the focus of a $f = 83.5$ mm ZnSe lens. The transmission is controlled with 100 μJ of 620 nm radiation focused on the semiconductor to a beam diameter of ~500 μm. This beam diameter is larger than the CO₂ spot size (<100-μm diameter) and ensures that no CO₂ radiation leaks outside the illuminated area. The arrival time of the visible pulse with respect to that of the IR pulse produced by the reflection switches is adjusted through a variable delay line (2-μm resolution). Si is used as the material for transmission switching mainly because its long absorption depth at 620 nm allows thick plasma layers to be formed, and therefore tunneling of the 10-μm radiation through the plasma is negligible. Any IR radiation transmitted through the Si is recollimated by using an Au mirror ($f = 35$ cm) and is sent in a shielded room in a He monitor ($f = 35$ cm) and is sent in a shielded room in a monitor on a 400-MHz HgCdTe detector.

All the semiconductor switches were controlled with a 70-fsec, 620-nm pulse obtained by amplifying the output of a colliding-pulse mode-locked dye laser⁹ in a XeCl pumped dye amplifier chain. The angular spread between the visible and the IR radiation is kept to a minimum to ensure that switching occurs at a constant phase front across the whole 10-μm beam diameter. The s-polarization of the 620-nm light ensures significant reflection (~80%) of the visible radiation from each CdTe surface, therefore leaving sufficient energy for the transmission switch.

The switched IR power is relatively low (~10⁴ W). Such power levels make standard autocorrelation measurements difficult to perform in the IR. An alternative method for measuring the IR pulse length is to determine the rise and fall times of the reflected and transmitted pulses by using cross correlation techniques.⁷ Experimentally, the transmitted CO₂ energy is monitored as a function of the time that the visible pulse takes to reach the transmission switch. The results of such an experiment are plotted in Fig. 2. The energy is measured on the 400-MHz HgCdTe detector that acts in the femtosecond time scale as a sensitive energy meter. Each point represents an average of 20 shots, and typical standard deviations are indicated. When the visible pulse arrives at the Si switch before the IR pulse, the transmitted energy is nearly zero, whereas the IR energy increases linearly for long delay time. (For the time scale of concern in this paper, the peak intensity of the CO₂ pulse can be considered constant.)

Fig. 3(a) and 3(b) provides evidence for the isolation of temporally modulated pulses (130 fsec) with fine modulation in the pulse structure through a saturated gain medium. Fig. 3(c) shows an autocorrelation trace of a 3 ps 10-μm regenerated, amplified pulse at its peak energy (after a small-signal-gain of ~40). Fig. 3(d) shows the autocorrelation trace of the same pulse after approximately 20 additional transits through the gain medium.

Since the lasing saturated amplification the temporal modulation has decreased substantially. These results are in qualitative agreement with theoretical calculations done by EFT. 7 for loose CO₂ resonators. If the temporal modulation was decreased as a result of gain saturation, spectral modulation peak area decreases. That is, there must be a spectral broadening mechanism. In Fig. 4(a) we show the spectrum of the peak pulse in the self-locked train. Figure 4(b) is the spectral equivalent to the autocorrelation trace in Fig. 3(d). Figure 4(c) shows the spectrum of a pulse late in the train equivalent to Fig. 3(e).

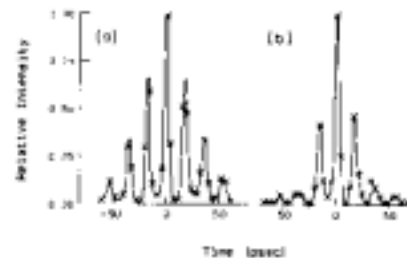


Figure 3: Autocorrelation trace of a regenerative amplified 130 fs pulse (a) at its peak energy and (b) after twenty additional transits through the gain medium. For these measurements the laser was operated on the 10 μm P branch.

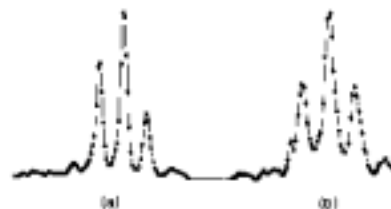


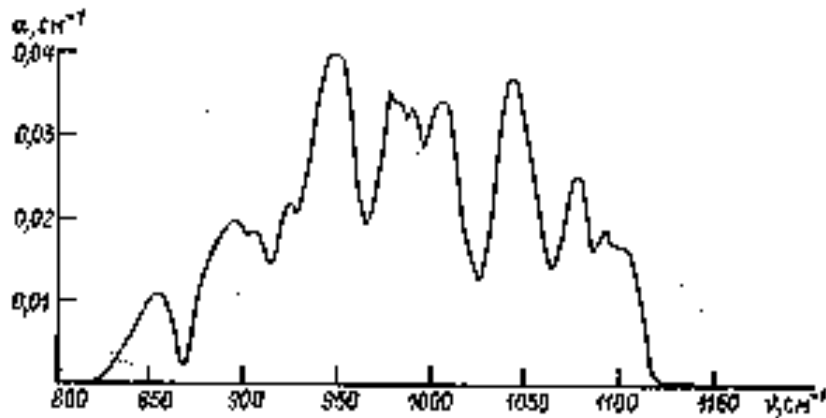
Figure 4: Spectra of (a) the regenerative amplified pulse at its peak energy and (b) a similar pulse after twenty additional transits through the gain medium. For these measurements the laser was operated on the 10 μm P branch with a 3 pass tapered pulse.

Clearly, gain saturation broadens the pulse spectrum in a self-locked CO₂ amplifier. The pulse in (b) and (c) was 7 ps in duration and the laser was operated in the 10-μm P branch. The pulse spectrum was obtained using an optical engineering spectrum analyzer and a silicon photodiode array. The hardware configuration was checked by combining use of the narrow $\lambda = 1.5$ μm diode with a $F = 1$ lens and a plane table output with 50% reflectivity. A CdTe photodiode array measured a single pulse from the output train. Pulses from different parts of the train could be probed by changing which diode between a beam-splitter spark gap and the photodiode unit.

Autocorrelation curves

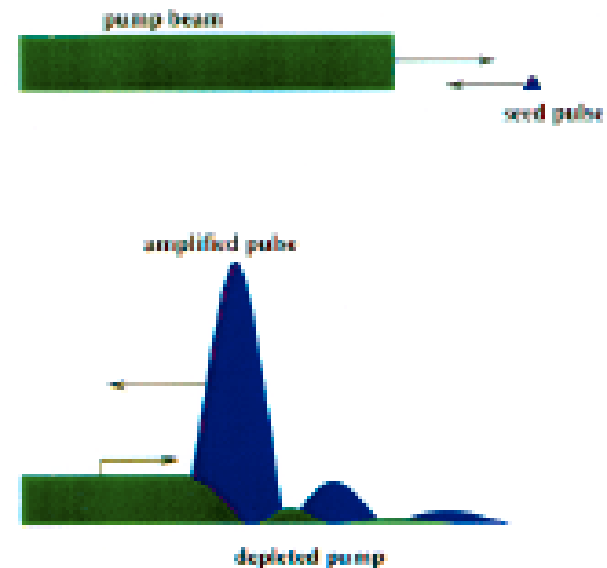
Some prospects for multi-Terawatt femtosecond CO₂ pulses

Direct amplification in a 4-atm CO₂ amplifier containing a mixture of molecular isotopes with ¹²C, ¹³C, ¹⁴C, ¹⁶O, ¹⁸O.
Gain bandwidth 7 THz sufficient for 150 fs pulse amplification.



Proposed by P. Corkum, V. Gordienko

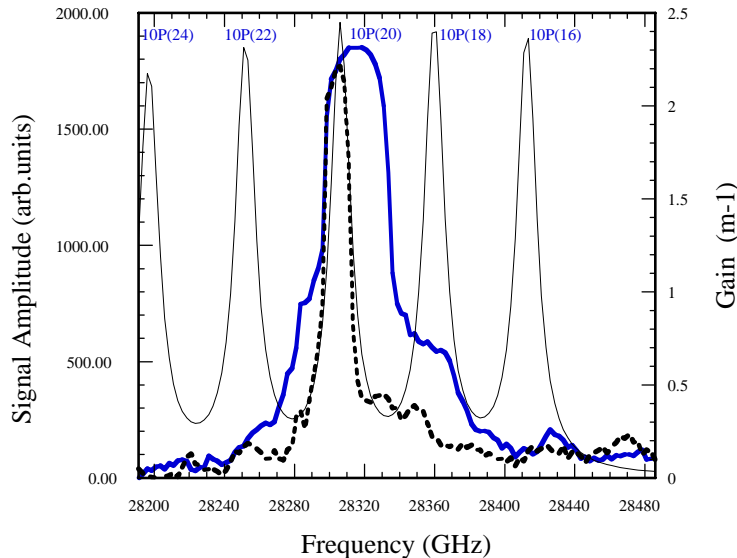
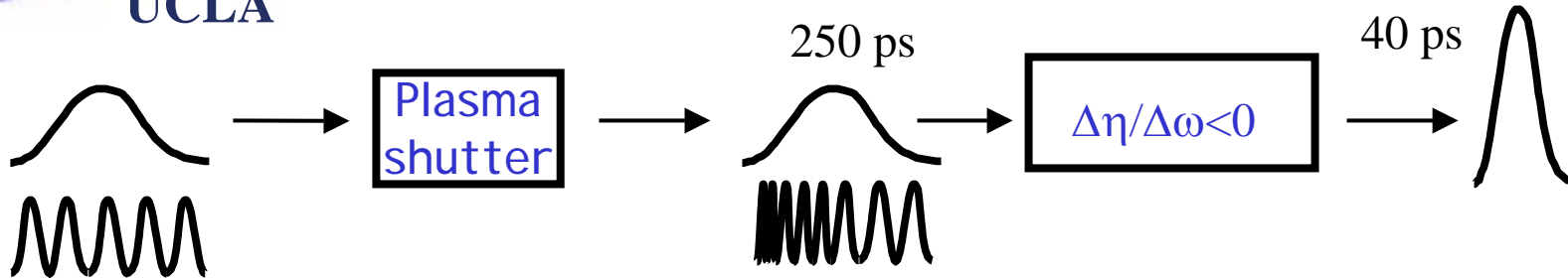
Raman backscattering of 9.6 μm nanosecond pump into counter-propagating femtosecond 10.6 μm seed pulse in resonance plasma $\omega_p = \Delta\omega$.
Possibility of high repetition rate as well.



Proposed by G. Shvets



Pulse Chirping and Compression in Laser Amplifier



Laser-induced ionization shifts the phase of the wave resulting in a chirp and subsequent pulse compression

$$\eta(x, t) = \sqrt{1 - n_e(x, t)/n_{cr}}$$

$$\Delta\omega = \frac{\pi n_e^0}{\lambda n_{cr}} \frac{\partial}{\partial t} \int n_e(t, x) dx$$

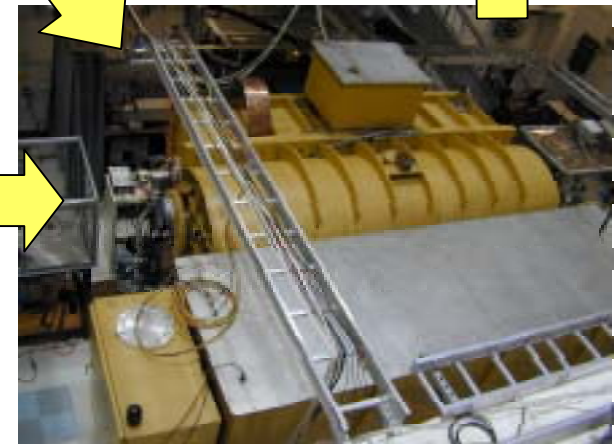
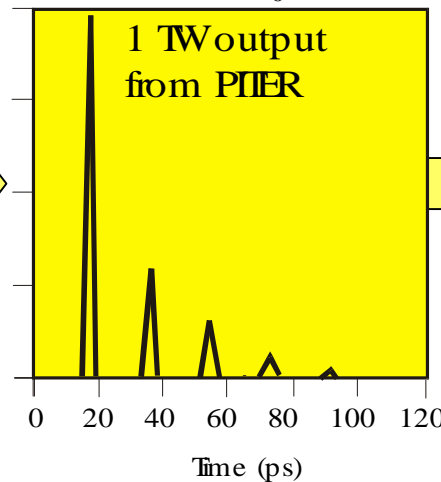
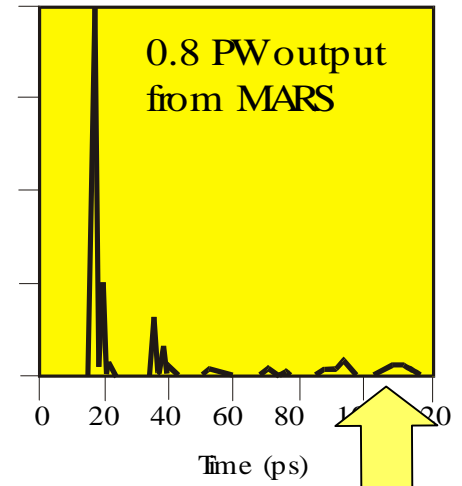
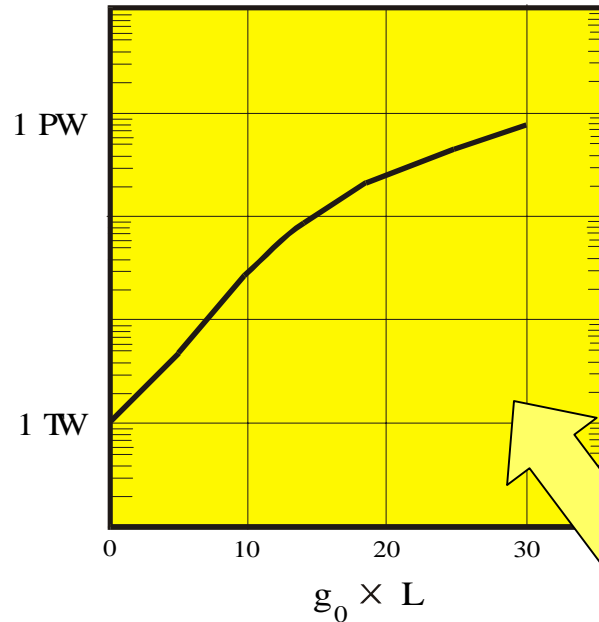
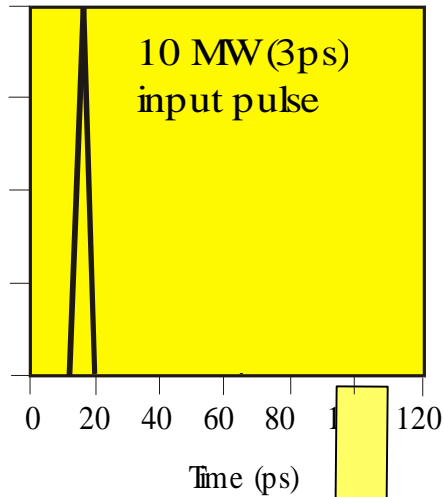
Measured blue shift 40 GHz corresponds to $n_e = 3 \times 10^{17} \text{cm}^{-3}$

Can be used to compress 1 ps to 100 fs

Hypothetical combination of PI TER with MARS provides 0.8 PW capability @ 1 ps

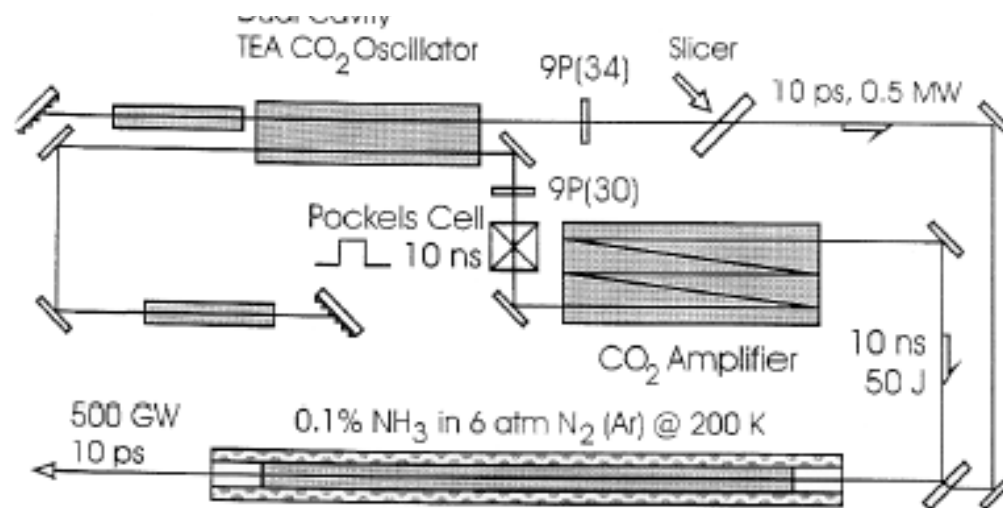
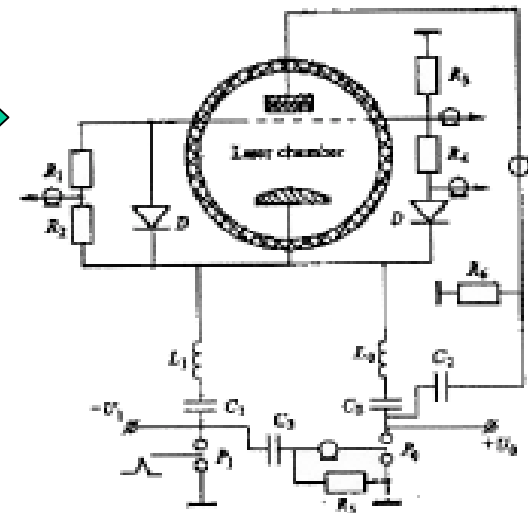
Use power or Stark broadening in laser field

$$\Delta \nu_R = \mu E / \hbar \quad , \text{ at } 10^{10} \text{ W/cm}^2 \quad \Delta \nu_R = 37 \text{ GHz}$$



Prospects for high repetition rate picosecond CO₂ pulses

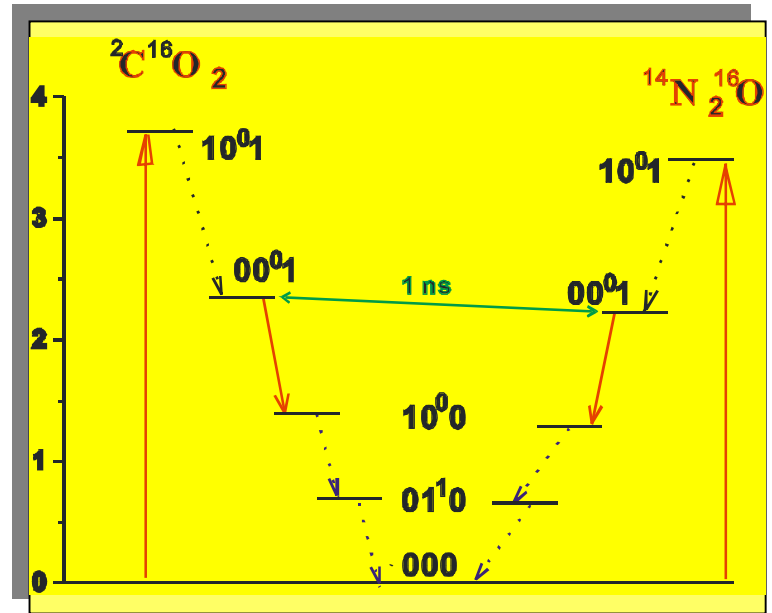
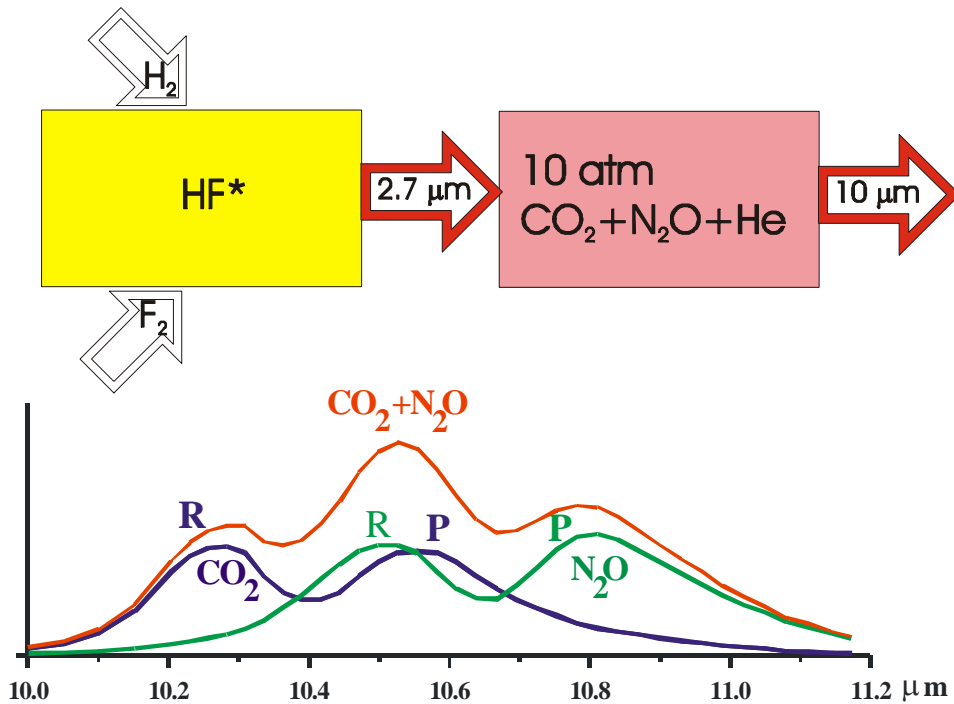
- ◊ X-ray preionized high-pressure gas discharge controlled by semiconductor switches
- ◊ Chemical pumping via energy transfer from DF to CO₂
- ◊ Optical pumping or energy transfer from nanosecond CO₂ pulses to picosecond laser pulses
 - ◊ 9 μm CO₂ laser pumping of 10 μm CO₂ transitions
 - ◊ CO₂ laser pumping of other molecular gases (NH₃)
 - ◊ Energy exchange between counter-propagating CO₂ laser pulses in plasma (G. Shvets)



Predicted: 60 dB gain at 3 J/cm², 10 ns pump CO₂ pulse*

*[J.D. White and J. Reid, *IEEE J. Quant. Electron.*, vol.29, 201 (1993)]

High-pressure CO₂:N₂O laser optically pumped by HF chemical laser



Demonstrated: Pumping Efficiency 20%, SSG 10%/cm

Another possibility is direct energy transfer via reactions
 $F + D_2 = DF^* + D$, $D + F_2 = DF^* + F$, $DF^* + CO_2 = DF + CO_2^*$

CONCLUSIONS

- ❖ Gas lasers potentially meet the requirements for advanced strong field applications (accelerators, radiation sources).
- ❖ Molecular and excimer gas lasers can operate in a parameter range for such applications including:
 - ❖ multi-TW peak power
 - ❖ ps or fs pulse length
 - ❖ ~kHz rep rate
 - ❖ ~kW or higher average power
- ❖ The closest fit to the aforementioned requirements CO₂ laser has also a fundamental attraction due to the λ^2 proportional ponderomotive potential.
- ❖ 1 PW CO₂ laser scheme is feasible within the present day technology capabilities. Focused to the diffraction limit with #F= 1, 1 PW produces field with a=70 (do not forget λ -proportional spot size too !) that allows realization of highly relativistic processes such as GeV ion acceleration, ponderomotive acceleration of electrons in a laser focus, study of Unruh radiation, etc.